



DETECTION OF BRAIN TUMOR IN MAGNETIC RESONANCE IMAGES

ANWAR A. BUFARES

JANUARY 2018

DETECTION OF BRAIN TUMOR IN MAGNETIC RESONANCE IMAGES

A THESIS SUBMITTED TO
THE GRADUATE SCHOOL OF NATURAL AND APPLIED SCIENCES
OF
ÇANKAYA UNIVERSITY

BY
ANWAR A. BUFARES

IN PARTIAL FULFILLMENT OF THE REQUIREMENTS FOR THE
DEGREE OF
MASTER OF SCIENCE
IN
COMPUTER ENGINEERING
DEPARTMENT

JANUARY 2018

Title of the Thesis: **Detection of Brain Tumor in Magnetic Resonance Images.**

Submitted by **ANWAR BUFARES**

Approval of the Graduate School of Natural and Applied Sciences, Çankaya University.



Prof. Dr. Can ÇOĞUN

Director

I certify that this thesis satisfies all the requirements as a thesis for the degree of Master of Science.



Prof. Dr. Erdoğan DOĞDU

Head of Department

This is to certify that we have read this thesis and that in our opinion it is fully adequate, in scope and quality, as a thesis for the degree of Master of Science.



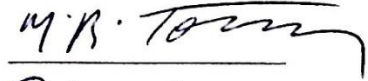
Assoc. Prof. Dr. Reza ASSANPOUR

Supervisor

Examination Date: 18.01. 2018

Examining Committee Members

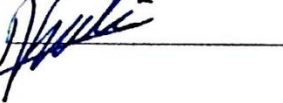
Prof. Dr. MEHMET REŞİT TOLUN (Aksaray Univ.)



Assoc. Prof. Dr. Reza HASSANPOUR (Çankaya Univ.)



Assist. Prof. Dr. Abdül Kadir GÖRÜR (Çankaya Univ.)



STATEMENT OF NON-PLAGIARISM PAGE

I hereby declare that all information in this document has been obtained and presented in accordance with academic rules and ethical conduct. I also declare that, as required by these rules and conduct, I have fully cited and referenced all material and results that are not original to this work.

Name, Last Name: Anwar BUFARES

Signature : 

Date : 18.01.2018

ABSTRACT

DETECTION OF BRAIN TUMOR IN MAGNETIC RESONANCE IMAGES

BUFARES, Anwar

M.Sc., Department of Computer Engineering

Supervisor: Assoc. Prof. Dr. Reza HASSANPOUR

JANUARY 2018, 62 pages

Brain tumor is one of the serious diseases that have caused death to many people in recent years. The complex structure of the brain and its main function associated with the central nervous system and its main role in controlling most of the functions of the body makes detection of tumor a challenging task. Many techniques have been presented in the medical field in order to detect brain tumor from MRI images. In this thesis, a system is designed to detect the tumor in brain Magnetic Resonance Imaging (MRI) using a seed-based region growing algorithm (SBRG) in the segmentation process. Then after segmenting the region of interest (ROI) the texture features are extracted from the image and used to classify tumor and non-tumor tissues by the implementation of the Artificial Neural Network (ANN) classifier. The accuracy obtained by this system is 99.88%.

Keywords: Magnetic Resonance Imaging, Gray Level Co-occurrence Matrix, Artificial Neural Networks, Seed Based Region Growing.

ÖZ

MAGNETİK REZONANS İMAJLARLA BEYİN TÜMÖRLERİNİN KEŞFİ

BUFARES, Anwar

Bilgisayar Mühendisliği Bölümü, Yüksek Lisans

Danışman: Doç. Dr. Reza HASSANPOUR

OCAK 2018, 62 sayfa

Beyin tümörü son yıllarda bir çok kişinin ölümüne neden olan çeşitli hastalıklardan birisidir. Vücutta işlevlerin çoğunu kontrol etmede merkezi sinir sistemi ve ana rolü ile beraber bulunan beyin ve ana işlevinin kompleks yapısı tümör keşfini tehdit eder. Bir çok Teknik, MRI imajlarından beyin tümörünü keşfedecek tıbbi alanda temsil edilir. Bu tezde, sistem; segmentasyon prosesinde tohum-esaslı bölgede-büyümeli algoritmayı (SBRG) kullanan beyin Manyetik Rezonans İmajlamada (MRI) tümörü keşfetmek için tasarlanmıştır. İlgili bölgeyi (ROI) segmentasyondan sonra, doku özellikleri imajdan çıkartılır ve Artificial Neural Network (ANN) sınıflama cihazı uygulaması ile tümürlü veya tümörsüz dokuları sınıflamak için kullanılır. Bu sistemin hassasiyeti (doğruluğu) %99 dır.

Anahtar kelimeler: Manyetik Rezonans Görüntüleme, Gri Seviye Birlikte Gerçekleşme Matriksi, Yapay Sinirsel Ağlar, Çekirdek tabanlı Alanın Büyümesi.

ACKNOWLEDGEMENT

First and above all, I would like to thank GOD for his never-ending grace and help that enabled me to finish my thesis successfully. "Without his support, nothing is possible".

I would like to express my immense gratitude to my Supervisor, Assoc. Prof. Dr. Reza HASSANPOUR, for his useful advices, valuable guidances, and continuous support in order to complete my research.

I would like to dedicate my success to my dear Father "Assanousi", and dear Mother "Salwa", whatever I say; I will not be able to express my thanks and gratitude for always surrounding me with love, support, and encouragement.

My heartiest gratitude to my husband "Mohamed" for his patient, understanding, motivation, and all sacrifices he made to help me during my study. Without his support I could not be able to get to this point. All the love to my wonderful twin babies "Anas and Leen", GOD bless them, Who were too young to understand why I was busy and spending a lot of time in front of my computer during the tenure of writing this thesis.

Finally, special thanks to my brothers and sisters "Nosiaba, Sukaina, Mohamed, Ala, Abdullah" and to my husband's parents "My second Father and Mother" and all his family for their endless love and encouragement.

TABLE OF CONTENTS

STATEMENT OF NON PLAGIARISM.....	iii
ABSTRACT.....	iv
ÖZ.....	v
ACKNOWLEDGEMENTS.....	vi
TABLE OF CONTENTS.....	vii
LIST OF FIGURES.....	viii
LIST OF TABLES.....	x
LIST OF ABBREVIATIONS.....	xi
CHAPTERS:	
1. INTRODUCTION.....	1
1.1. Problem and Motivation.....	1
1.2. Thesis Objective.....	2
1.3. Contributions.....	2
1.4. Scope of Thesis.....	4
2. LITERATURE SURVEY.....	5
2.1. Image Segmentation Techniques.....	5
2.1.1. Thresholding Methods.....	5
2.1.2. Region-based Methods.....	9
2.1.3. Edge-based Methods.....	13
2.1.4. Clustering Methods.....	17
2.1.5. Classification Methods.....	20
3. PROPOSED METHOD.....	29
3.1. Proposed System.....	29
3.1.1. Preprocessing.....	31

3.1.2.	Divide Image into Blocks.....	33
3.1.3.	Feature Extraction.....	33
3.1.3.1.	Mean of blocks.....	34
3.1.3.2.	Haralick Texture Features.....	34
3.1.4.	Feature Selection.....	36
3.1.5.	Classification.....	37
3.1.6.	Seed Based Region Growing Algorithm.....	40
4.	EXPERIMENTAL RESULTS.....	41
4.1.	Data Source and Used Tools.....	41
4.2.	Proposed Method Experiments.....	42
4.2.1.	Preprocessing.....	42
4.2.2.	Divide Image into Blocks.....	44
4.2.3.	Feature Extraction.....	45
4.2.4.	Classification.....	46
4.2.5.	Segmentation.....	48
4.3.	Evaluation.....	53
5.	CONCLUSION AND FUTURE WORK.....	57
5.1.	Conclusion.....	57
5.2.	Future Work.....	58
	REFERENCES.....	59

LIST OF FIGURES

FIGURES

FIGURE 1 Block Diagram of the Designed System.....	3
FIGURE 2 Flowchart Diagram of the Proposed Methodology.....	30
FIGURE 3 The Steps of Preprocessing Stage.....	31
FIGURE 4 Histogram of Original and Normalized Image.....	32
FIGURE 5 Block Diagram of Feature Extraction sub steps.....	33
FIGURE 6 The Structure of the Neural Network.....	37
FIGURE 7 Snapshot of ROC in the Training Stage.....	38
FIGURE 8 Snapshot of Confusion Matrix in the Training Stage.....	39
FIGURE 9 Snapshot of Performance in the Training Stage.....	39
FIGURE 10 Region Growing Process.....	40
FIGURE 11 Snapshot Histogram of 00005-IM Original and Normalized Image.	42
FIGURE 12 Snapshot Histogram of 00001-IM Original and Normalized Image.	43
FIGURE 13 Snapshot Histogram of 00025-IM Original and Normalized Image.	43
FIGURE 14 Snapshot of Divided the Image.....	44
FIGURE 15 Snapshot of MRI Image (000005-IM) Showing Tumor Position.....	46
FIGURE 16 Snapshot Show the Result of (000018-IM) After SBRG.....	48
FIGURE 17 Snapshot Show the Result of (000005-IM) After SBRG.....	49
FIGURE 18 Snapshot Show the Result of (0000025-IM) After SBRG.....	49
FIGURE 19 Snapshot Show the Result of (000014-IM) After SBRG.....	50
FIGURE 20 Snapshot Show the Result of (000020-IM) After SBRG.....	50
FIGURE 21 Snapshot Show the Result of (000021-IM) After SBRG.....	51
FIGURE 22 Design of Graphical User Interface 1.....	51
FIGURE 23 Design of Graphical User Interface 2.....	52
FIGURE 24 Confusion Matrixes.....	53

LIST OF TABLES

TABLES

Table 1: Part of the Selected Feature Extraction Results and their Class Attributes.....	45
Table 2: Shows Part of Classification Result for (000005-IM) Image.....	47
Table 3: Proposed System Statistical Values.....	54
Table 4: Calculation of Evaluation Metrics.....	55
Table 5: Evaluation of Proposed System.....	55
Table 6: Comparison of Various Segmentation Methods.....	56

LIST OF ABBREVIATIONS

IARC	International Agency for Research on Cancer
WHO	World Health Organization
MRI	Magnetic Resonance Imaging
ROI	Region of Interest
ANN	Artificial Neural Network
SRGA	Seeded Region Growing algorithm
ABTS	Automatic Brain Tumor Segmentation
T1	T1-weighted image
T1C	T1-weighted gadolinium contrast agent
T2	T2-weighted image
FLAIR	Fluid Attenuated Inversion Recovery
GTV	Gross Tumor Volume
RFCM	Region based Fuzzy C-Means Clustering Method
CSF	Cerebrospinal Fluid
GM	Gray Matter
WM	White Matter
MCD	Minimum Covariance Determinant
kNN	k Nearest Neighbor Classifier
GLCM	Grey Level Co-occurrence Matrices
IKFCM	Improved Kernel Fuzzy C-Mean
FPCM	Fuzzy Possibilistic C-means
TP	True Positive
FP	False Positive
3D	Three Dimensional
FLICM	Fuzzy Local Information C-means

SVM	Support Vector Machine
T1post	T1 weighted post-contrast
DICOM	Digital Imaging and Communications in Medicine
MI	Mean Intensity
HOG	Histograms of Oriented Gradient
LBP	Local Binary Pattern
TPR	True Positive Rate
FPR	False Positive Rate
ROC	Receiver Operating Characteristic
DSS	Dice Similarity Score
CAD	Computer Aided Detection
FPCNN	Feedback Pulse-Coupled Neural Network
PCA	Principal Component Analysis
BPNN	Back Propagation Neural Network
HE	Histogram Equalization
CE	Contrast Enhancement
TCIA	The Cancer Imaging Archive

CHAPTER 1

INTRODUCTION

1.1 Problem and Motivation

Today Cancer has become a serious and diffuse disease that causes death to many people all over the world. The International Agency for Research on Cancer (IARC) reports that have been made in 2012 indicates that there were about 14.1 million new cancer infections and also 8.2 million deaths because of cancer worldwide. Also due to the population growth it expects that the global burden will increase to 21.7 million new cancer infections and 13 million deaths of cancer by the year 2030 [1].

Brain tumors are considered as one of the most dangerous types of cancer that leads to death of children and adults under 40. It has been found that children, women under the age of 35 and men under the age of 45 are killed by brain tumors more than other type of cancer like leukemia, breast and prostate cancers [2].

According to the facts presented by the World Health Organization (WHO) about 30–50% of cancer cases can be prevented and reduced by being aware of the risk factors that cause cancer therefore avoiding them. Also early detection of cancer plays an important and effective role in decreasing cancer mortality. Patients can have a high chance of survival where tumors can be more controlled in their initial stages in many cases [3].

In order to detect tumors in early stages, medical image technologies are used in the medical field to help doctors to diagnose and identify the presence of abnormal cells. Magnetic Resonance Imaging (MRI) is considered as an efficient tool in brain imaging that provides good results due its ability to distinguish between different brain tissues. In addition, computer-aid systems in turn increase the probability of early detection where they can help physician to determine whether the patient needs treatment or undergo surgery.

In this thesis, a brain tumor detection system will be introduced to facilitate the work of radiologist's to detect and classify the abnormal cells.

1.2 Thesis Objective

The main goal of this thesis is to design and evaluate an automatic brain tumor detection system. This system is supposed to determine and detect the Region of Interest (ROI) and extract the tumor from MRI images.

The system is simply designed to be used as preliminary work to develop a fully automatic detection system that detects the suspicious region from other great diversity of normal tissues in the brain in order to help physicians and radiologists to facilitate their tasks.

1.3 Contributions

- In this study, a brain tumor detection system was proposed in order to detect tumors in MRI images. The method goes through four stages: At first, we perform standard grayscale normalization to all MRI images (512 x 512 pixel size) which is important as a preprocessing step to reduce the illumination effect and easily distinguish between different brain tissues.
- In the second stage, each image is divided into 8 x 8 blocks and then we calculate the 13 Haralick Texture Features for all blocks including normal and abnormal parts. After that we select the ones that give better results in order to build the Artificial Neural Network (ANN) classifier.
- Third stage includes the design of the Artificial Neural Network. The network consists of two major steps. At first, a classifier is trained by using the extracted features of specified candidate regions from normal or abnormal regions of training data. These features are used as the input neurons with their class attributes in order to get the weights of the network. Secondly, the trained classifier is performed on the testing data to verify tumor and non-tumor blocks for all tested images. Finally the obtained results of the network which were

classified in the truly class (TP) are used to determine the seed points of the region growing algorithm in the next stage.

- In the last stage we used a Seeded Region Growing algorithm (SRGA) to separate the area of the tumor from other brain components. The seed point of each image is chosen based on the classification result of the neural network, where those blocks that contain the tumor are considered as candidate seed points.

The following Figure 1 shows the stages of the proposed system to detect the tumor.

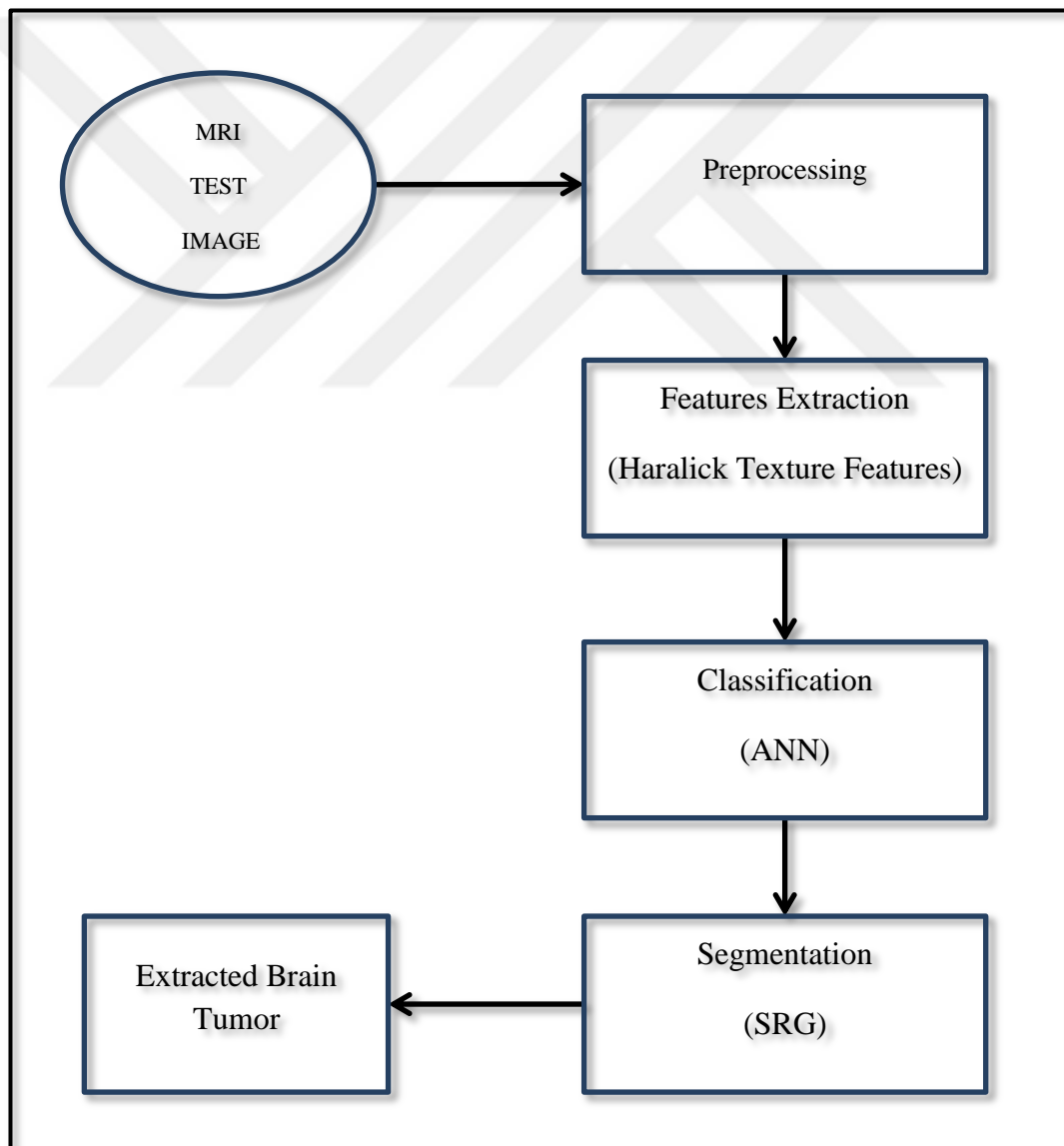


Figure 1: Block Diagram of the Designed System

1.4 Scope of Thesis

The next chapters in this thesis are described as follows:

Chapter 2: Literature Review, a survey on work done by other researchers in the field of MRI brain tumor detection is introduced in this chapter, where a detailed description of each segmentation and classification technique is presented mentioning the strong and weak point of each method.

Chapter 3: Proposed Method, this chapter presents a description of the data that have been used in our study and a fully discussion of the four stages of the proposed system.

Chapter 4: Experimental Results, the outcome of the proposed system has been given with snapshots stating the final segmentation results and also the evaluation of the system performance are presented.

Chapter 5: Conclusions and Future Work, concludes the work that have been done based on the obtained results and performance evaluation and suggest some tips and plans for future works.

CHAPTER 2

LITERATURE SURVEY

A large diversity of different tumor detection and segmentation approaches using medical images have been proposed and published which have its own suppositions, advantages, and limitations. In this chapter, a review of previous studies done by other researchers is introduced. Various segmentation techniques and algorithms for brain tumor detection using MRI images are reviewed and discussed mentioning the advantages and drawbacks of each method.

2.1 Image Segmentation Techniques:

2.1.1 Thresholding Methods:

Threshold method is one of the simplest techniques that can be used in image segmentation. This technique is performed by converting a gray scale image into a binary image. The main idea of this technique is to select a threshold value (T) to separate one or more object in the image. In this method the gray level values which are below the threshold is considered as 0 (black) and the others above the threshold is considered as 1 (white). Two types of thresholds are used in image segmentation depending on the number of the objects in the image. Where a single threshold is used when the input image contains one object and a multi threshold is used when the image contains more than one object. Thresholding technique is presented and discussed in this section.

1. In this paper [4], Idanis Diaz et al. proposed an automatic brain tumor segmentation (ABTS) tool in order to segment different brain tissue components. Four types of magnetic resonance images were used: T1-weighted image (T1), T1-weighted gadolinium contrast agent (T1C), T2-weighted image (T2) and Fluid Attenuated Inversion Recovery (FLAIR). A multi-thresholding based histogram technique depending on geodesic dilation morphological operator was used. The proposed method contains four stages: Thresholding, Skull Segmentation, Edema Segmentation, and GTV Segmentation. The main objective of this work is to find both the edema and gross tumor volume (GTV). In Thresholding stage the writers of this paper have clarified the common bimodal histograms in brain MRI which are:

- 1) First mode denotes the intensity values close to zero which are found in the background of the image.
- 2) Second mode consists of grey values which are found in the brain tissues belonging to gray and white matter.

The researchers obtained a binary 3D masks by localizing different thresholds in the histogram images in order to separate the tumor region from MRI images, such as background from foreground, or region of interest consisting low/high intensity levels from other healthy tissues. They used a smoothing filter to get smooth histogram envelopes in order to facilitate the threshold localization. After obtaining the smooth histogram envelopes, the first and second histogram modes are localized (μ_1 , μ_2). Then three main thresholds were marked after the second mode μ_2 , so high intensity areas can be separated from other brain tissues. These thresholds were defined as:

T A: the maximum slope change point.

T B: the first slope change of the intensity value which is greater than TA.

T Fgr: the first slope change found on the left of the μ_2 .

A 3D image based on MRI modality was then presented and used with a threshold to define the 3D mask which is given as: $M(m, T)$, Where M indicates the mask, m indicates the MRI modality, and T is the threshold. For instance the mask $M(T_2, TA)$ includes all T2 voxels with intensities greater than TA. In skull segmentation an initial approximation of skull location was presented to obtain a mask skull which includes just the skull. This mask was then used to remove the skull from MRI threshold modalities.

In edema segmentation a geodesic dilation operator and two masks $M(\text{FLAIR}, \text{TA})$, $M(\text{FLAIR}, \text{TB})$ belonging to the edema are used. The first mask $M(\text{FLAIR}, \text{TA})$ contains some regions which don't belong to the tumor while the other $M(\text{FLAIR}, \text{TB})$ contains less parts of the edema. Due to that, ABTS used the edema of the $M(\text{FLAIR}, \text{TB})$ mask as a seed point for the geodesic dilation operator until all area of the edema was covered in $M(\text{FLAIR}, \text{TA})$. In some cases when the edema is not completely extracted ABTS performs the geodesic dilation operator after the intersection of both $M(\text{T2}, \text{TA})$ and $M(\text{FLAIR}, \text{TFgr})$. Where T2 contains voxels with high intensity values belonging to the edema and Fgr threshold separates all other regions containing low intensities. In order to achieve precise results, geodesic dilation operator used $M(\text{FLAIR}, \text{T})$ in addition to the information presented by T2. Last stage in this study was GTV Segmentation where the threshold of T1C MRI image was used to identify the GTV as well the information provided by a voxel-wise intensity subtraction of T1 from T1C ($\text{IT1C}-\text{T1}$). At first the intensity values was standardized to cancel the regions which not belongs to the tumor tissue. Then voxels with high intensities was selected from $\text{IT1C}-\text{T1}$ and the edema mask which was deduced in the previous stage.

The segmentation results of the proposed work achieved an average Dice accuracy of 81% for edema segmentation and 85% for gross tumor volume segmentation.

These results show that the proposed ABTS method works very well and gives accurate results also computation time was fast. Threshold methods are easy implemented and previous information are not need, but on the other hand this method has some disadvantages as the limited ability to enhance the tumor regions where it's usually used as a preprocessing technique in other segmentation methods. Also it completely depends on histogram peaks in order to find the required threshold value. The threshold selection is not that easy where the spatial information of pixels is not included.

2. During their research, Paternain et al. [5] submit a new thresholding algorithm to segment MRI brain images. This algorithm depends on the incomparable concept where the main object is to find a threshold for pixels with no incomparability between background and other image classes. The researchers in this paper relied on two main operators to build the fuzzy sets of the algorithm which were the mean intensity level and the membership value of each background and objects. Then the optimal threshold value was computed using the incomparability degree with the help of expert determining whether the membership of intensity belongs to the object or the background. The accuracy evaluation was done by using the incorrectly classified voxels percentage. Two experimental studies were presented and T1-weighted MRI images were used:

a) Slice by slice segmentation: This compares the proposed algorithm with Otsu's local thresholding algorithm. This experiment contains two steps. In the first step a local threshold was computed for 13 MRI brain images each one contains 41 slices to segment the white and gray matter. The second step is computing the percentage of 41 slices which contains incorrectly classified voxels. The obtained results showed that in all images the proposed method achieved smaller percentage numbers than Otsu's.

b) Global segmentation: in this experiment the proposed algorithm was compared with Otsu's global thresholding. A single histogram was calculated for all 41 slices of the same image in order to find a global threshold using the algorithm. Then the percentage of bad classified voxels was computed. In this experiment the obtained results showed that the proposed algorithm achieved small percentage numbers than the Otsu's global threshold.

Experimental studies proved that results achieved by using global segmentation in both proposed and Otsu algorithms were better than using local segmentation.

This proposed work has some advantages where it gives clear and good results compared with expert's manual segmentation results. The global thresholding method which gives better result has the advantages of simple implementation and also is commonly used in medical images. Also segmentation using local threshold gives good result where in some cases it's used to improve the global threshold as it happened in this research study. Disadvantages of this algorithm are that thresholding is widely used in various segmentation methods as an initial step.

In other words, thresholding algorithms are considered as a limited tool that could separate the entire tumor from the image. Also using thresholding method as an initial step in some segmentation methods could lead to high FPs and FNs rates.

2.1.2 Region-based Methods:

Region based methods are those methods which merge pixels that have same the properties in an image. This approach works by checking and joining the neighboring pixels of a sub area into large areas according to some specific criteria defined by the used method. Watershed and Region Growing are the most frequently region based methods that are used in the medical field especially for brain tumor segmentation.

A discussion of both region based methods is described below:

1. Jun Kong, et al. in [6] proposed a novel approach for segmenting different brain tissues in MRI (Magnetic Resonance Imaging). The aim of this method is to produce a robust and very accurate segmentation. The proposed approach composed of four sections. In the first section noise of MRI images is removed. Since there are different levels of noise in medical images an adaptive wavelet based filter is applied in order to achieve good results.

This algorithm performs a preliminary coefficient classification by using the valid knowledge of the correlation of image features via resolution scales. The method provides a useful image features on one side and mainly noise on the other by estimating the statistical distributions of the coefficients giving the desired results.

The second section is to apply a watershed algorithm to segment the brain tissues as an initial segmentation process. The used mechanism in this method is immersion simulation which produces segmented MRI images having non-overlapping regions. This method is considered as one of the best methods but it causes some problems such as over-segmentation and some of the regions in the image as transitional parts are not completely divided.

Third section is a merging process where a region based Fuzzy C-Means clustering method (RFCM) has been applied to overcome the problem of over segmentation regions in the previous section.

This method works by merging the regions with similar properties in order to reduce the number of over-segmented regions. The merging process is obtained by allocating each region to a class using a membership value. Where the regions are clustered into 3 classes which are indicated by the number of tissues of interest (cerebrospinal fluid (CSF), gray matter (GM), and white matter (WM)) included in this study. After using the RFCM clustering method the resulted image showed that some regions were still not segmented completely.

Section four is a re-segmentation processing approach to detect and segment the transitional regions which are not partitioned completely. This approach consists of two main steps. First step is detecting the re-segmented regions by using a fast Minimum Covariance Determinant (MCD) estimator and second step is to split these regions that needed to be re-segmented by using the classical k nearest neighbor (kNN) classifier. Variance and mean value are considered in this approach to determine the inhomogeneous regions. Where the variance of inhomogeneous regions are higher than the homogeneous ones and also the inhomogeneous regions can be identified by mean value if the mean value was found far from the center point of the class it belongs to.

In the first step MCD estimator is applied by removing the outlier dots, which are considered as the transitional regions that need to be re-segmentation, leaving the inliers ones which gives the optimum result of the RFCM clustering. The inliers regions are also used as a training set in the next step. The second step is utilizing the kNN classifier to divide regions that need to be re-segmented. The kNN classifier computes each point nearest k training feature space samples and then classified them using the label most represented between the k closest neighbors.

As a result, this paper presented a novel approach that produced a robust and highly accurate brain tissue segmentation compared with other segmentation methods. The combination of using Minimum Covariance Determinant estimator and k-Nearest Neighbor classifier gives a very good result due to the ground truth. Watershed algorithm was used by researchers in this approach due to its advantages represented in the simplicity and low computation time. Another advantage of using watershed algorithm is that it provides a complete division of an image. But on the other hand, watershed algorithm has some disadvantages such as over-segmentation and some regions were not completely divided clearly appear in the transitional regions in the

image between the gray matter and white matter or gray matter and cerebrospinal fluid. Consequently, the following methods: Fuzzy C-Means clustering algorithm, Minimum Covariance Determinant estimator, and k-Nearest Neighbor classifier have been applied to overcome these drawbacks.

2. Wu et al. in [7] described a texture feature based on seeded region growing technique for an automatic image segmentation of medical MRI images. A combination of two different textural features was used. In their work, first a Co-occurrence texture feature and Semi-variogram texture feature are used in order to get the feature spaces and then the automatic seeded region growing algorithm was applied. In the first part of the Feature Extraction, researchers computed the grey level co-occurrence matrices (GLCM) which was first proposed in 1973 by Haralick [8]. It was computed by square dimension N_g that represents the number of grey levels in the image. After that they calculated the 14 statistics of the GLCM for each pixel in four directions. In the second part a semi-variogram feature was extracted from all pixels in the region of interest (ROI). This process consists of two points:

- a) Using the mean Square-Root Pair Difference to compute the semi-variogram where a 3×3 neighboring window, Four variogram directions (0° , 45° , 90° , 135°) and one distance $d=1$ are computed for each pixel.
- b) Converting the directional features to rotation-invariant features.

After Co-occurrence and semi-variogram texture features were extracted a seed point is determined depending on a cost-minimization method. This cost function consists of three sub-functions based on three factors related to the seed point which are:

- a) The seed must be inside the region and also close to the center.
- b) The seed point feature must be close to the average of the region.
- c) The distances between the seed pixel and neighbors should be small to insure continuing the growing process.

Equal weights were then given for the three sub-functions in order to apply the cost function on the ROI pixels where the pixel with minimum value was considered as the seed point.

The next step of this methodology was Region Growing Method where seed point's neighbors were checked to see whether they belong to the same region or not. If they belong to it the neighbors of them are also checked recursively until no more neighbored pixels have the same properties in the region.

Last section in this work was threshold value optimization. The purpose of this step is finding the value with the highest threshold just before explosion where this value is called the optimal threshold value. The region growing start from a low threshold value (seed point) and then increases it by 1. For each threshold they applied a SRG algorithm and then evaluated its result. The segmentation starts automatically once the ROI is selected without any user intervention where in the seed point determination, the cost function evaluates all pixels in the ROI and the pixel which is found with the minimum cost is considered as the seed point. In the threshold determination method, threshold values are examined from the starting value and then SRG was applied to choose the exact threshold value. Segmentation results showed that semi-variogram based SRG is better in terms of saving time because co-occurrence based SRG requires a co-occurrence matrix for each pixel and then 14 statistics has to be compute while features of semi-variogram are extracted immediately from neighboring window.

The advantages of this work are that it reduces the user intervention and it also overcomes the explosion and over-segmentation problems. Region growing method is useful because it easy defines and segments the regions with similar criteria's. However, this method has some disadvantages. Region growing could result in holes and over segmentation problems because of the variations in pixel intensities of the image. Consequently, post-processing are required for the segmentation results. Moreover, some pixels inside the region are left because of homogeneity problem but on the other hand, this can be helpful to detect tumors inside organs.

2.1.3 Edge-based Methods:

Edge based segmentation methods are used to clarify the edges of an object found in an image. The aim of this approach is to determine the closed boundaries of an object, which is defined as a series of linked pixels, so that the boundary among two regions with different gray-level properties can be located and separated. This technique is commonly used in MRI images because of its sensitivity and ability of finding the brain tumor boundaries.

A scope of edge based methods as closed contour algorithm, parametric and geometric deformable models are presented and discussed as follows:

1. W. Yang and M.Siliang in [9] used a fuzzy classification and parametric deformable models to present an automatic brain tumor detection and segmentation method. This method contains a combination of two classification techniques: region based and contour based in order to get more precise classification and segmentation results. MRI (magnetic resonance images) of brain tumor which includes different weighted sequences and shows the different characteristics of brain tissues was used. At first the brain MR image was segmented by a new method that determines the presence of tumors cells. Then an improved Kernel Fuzzy C-Mean classification method (IKFCM) which is a combination of Kernel and Fuzzy C-Means method was applied with Morphological operations as an initial stage. Where the IKFCM method was considered as one of the best fuzzy clustering methods that gives a good segmentation performance than others. In this stage for tumor detection a histogram analysis based IKFCM was utilized in order to obtain the initial value to avoid the initialization problem of classification. The extracted image from the brain was categorized into five main classes: white matter, gray matter, cerebrospinal fluid (CSF), tumor, and background. The researchers of this paper used the mean for each of gray matter, white matter, and cerebrospinal fluid as centers for their classes. The zero value was used for the background while the tumor class has the highest intensity among all five classes. After tumor was detected and classified from other brain parts some morphological operations, for instance (largest component selection, opening, and erosion) was then implemented to the tumor region to correct any misclassification errors were found.

In the second stage of the proposed method tumor segmentation process was done by applying a parametric deformable model to segment the internal parts of the brain. Where the output of the previous process (IKFCM implementation) was used as the initial input value for deformable method in order to get the desired, precise segmentation result.

A quantitative evaluation to improve the segmentation results was done by comparing the results of the proposed method with the results of a fuzzy possibilistic c-means method (FPCM) on fully enhanced tumors types. Two evaluation measurements were used true positive (Tp) that indicates ratio of the correct tumor detection and false positive (Fp) that indicates the ratio of false tumor detection. The comparative quantitative evaluation shows that the proposed method achieves better results than the fuzzy possibilistic c-means method and also gives a high segmentation quality results.

This work has an advantage of using the combination of region based and contour based methods that gave a good segmentation result by taking the benefits of both methods and eliminating their defects at the same time. Another advantage was the application of the proposed method on different brain tumor datasets achieved a high segmentation results wherever the tumor was located or different in sizes and shape.

One of the disadvantages of this work that there are not any specific techniques or standard images used in the evaluation section; therefore, more tests and auditing are needed to verify the authenticity of the proposed method and improve its robustness. Also IKFCM can only be used as an initial step to detect the tumor because it shows only a part of the tumor not the whole tumor; and according to that a second segmentation method must be used which is (Deformable Model) that results in showing the entire tumor. Parametric deformable model has some disadvantages represented in its topology dependent, which mean it cannot handle the topological changes thus a model can only deal with a single ROI and can cause to wrong boundary covering in case of inhomogeneities [10].

2. Sean Ho, Elizabeth Bullitt, and Guido Gerig, in their study [11], have provided an automated (3D) MRI segmentation method. The researchers in this work combined both level-set and region competition methods. Since Level-set method faces the problem of determining the initial contour and can lead to having missing parts of boundaries, authors used region competition to overcome these problems and give more reliable and accurate results. They used pre- and post-contrast T1 weighted MRI images in order to estimate the probability map of the tumor. They used the force factor of the image to modify the level-set snakes propagation term in the range of -1 and $+1$ so the snake expand or shrink whether its inside or outside the tumor, respectively. They also applied a Gaussian smoothing by adding a term to the snake evolution function in order to avoid any noisy structures in the image and to obtain the numerical stability of the method. After that an intensity classification (Tumor Probability Map) was done to classify the voxels which ones belong to the tumor and which belongs to the background. Then a histogram was fitted using the difference between both pre- and post- T1 weighted by Gaussian and Gamma distributions. The propagation term of the enhanced tumor part was resized to the range $[-1, 1]$ and used as the probability map to guide the level set snake. Finally the initialization of the probability map was done by adjusting the level set to 0 and the implicit function was initialized using the initial contour leading to the full automatic snake initialization. The method was compared with expert's manual segmentation and achieved good and successful results on different tumor datasets.

If we want to discuss the advantages of this algorithm in a comparison with parametric deformable models, Level set methods are easy implemented, non-parametric, accurate, and powerful modeling tool. It also has the ability to handle the sharp corners in complicated shapes in the propagation term even with topology changes.

On the other hand, the proposed method has some drawbacks that it depends on a precise tumor probability map where any mistake in the initialization process could lead to weak or inaccuracy results because the intensity differs from a tumor to another. Furthermore, the computation cost of this algorithm is high.

3. In the paper of [12] Asra Aslam, Ekram Khan, and MM Sufyan Beg discussed an improved brain tumor segmentation method. This study is based on Sobel detection, and Closed Contour Algorithm to extract the tumor from the image. The researchers compared their work with other conventional methods as Sobel edge detection and thresholding methods. In their proposed segmentation method first, in order to get the gradient of the image Sobel Operator is used. A 3x3 mask is applied on the image and then gradient is calculated and defined. The second step is locating the tumor edges by finding a threshold value automatically. As soon as the final threshold is determined, this threshold was compared with each gradient image pixel were pixels with high gradient were specified as a white pixel (edge point); otherwise it's considered as black (background point). Third step is closed contour method where a seed point is determined for each region and then it is expanded using the mask in first step in order to find region pixels which are not edge ones. Then connected pixels neighbors are checked if they belong to the same region or not. This process continuous iteratively until the pixel inside the window was found as a boundary pixel. Finally, segmentation process is done to separate the brain tumor from the image. The tumor is extracted by deciding the most active region in the image which is considered as the brighter color part. After tumor segmentation the result obtained by proposed method was compared numerically with Sobel and watershed approaches. The comparison indicated that the final segmentation result achieved by improved edge detection method is better than other two approaches and the extracted tumor region is closer to the original image. Edge detection methods are commonly used due to the easy implementation and detection of the object edges. Improved edge detection method has some advantage over other conventional edge methods where simulation results showed that proposed method have determined most closed contours of the tumors in all tested images.

From our point of view the combination of Sobel and closed contour methods worked very good and achieved more accurate results against Sobel and watershed methods. These conventional approaches have some disadvantages where they are not accurate enough to give good closed contours results. They are sensitive in some cases to noise and threshold values especially in complex images as MRI images.

2.1.4 Clustering Methods:

Clustering techniques have been widely used in the image segmentation domain.

The clustering process is a selective procedure in which similar data pixels in an image are joined and grouped together into one cluster and other different data pixels are grouped into different clusters depending on similar properties. The centroids of each cluster are then used to classify image patterns, where each pattern is assigned to the closest centroid. Different clustering techniques are presented in this section:

1. The writers of this paper [13], Abolfazl Kouhi, Hadi Seyedarabi, and Ali Aghagolzadeh, presented a modified fuzzy c-means algorithm for segmenting MRI brain images. This algorithm was proposed to overcome the problem of noise sensitivity of the original FCM algorithm where spatial information is not taking into consideration. The standard fuzzy c-means algorithm was first mentioned and compared with the hard c-means method. FCM clustering method retains more information of an original image which is an important property but, on the other hand, it doesn't utilize the spatial information of that image. The spatial relationship between pixels plays an important role particularly in image segmentation where neighboring pixels are interconnected and almost has the same data features. In FCM algorithm the objective function was minimized because of using iterative operations in order to get the cluster centroids and membership functions values. The objective function gives low objective values when data points close to the centroid of their clusters are assigned high membership values; conversely, high objective values are given when data points far from the centroid of their clusters assigns low membership values.

The second part is the modified FCM algorithm where the team of this paper found that a common parameter α was shared by some modified FCM algorithms as FCM_S1, FCM_S2, FCM_S and EnFCM. The selection of this parameter is very important in order to make balance between each of the intensity to noise and the ability to retain details for an image. The value of α is usually small for those pixels with little or no noise corruption. In this case, adjusting the neighboring pixels which has the same α value in an image during the segmentation process will be unreasonable. Therefore, the researchers of this paper modified a fuzzy local information c-means (FLICM) algorithm to avoid this problem.

Where they took the advantages of FCM approaches and canceled its drawbacks by updating each of cluster centroids and membership functions and exploit the spatial information property taking into account these two points:

(1) In the spatial pixel relationships if the window size was widened then α value should be adjusted to a different space from the window center, or blur will be occurred in the image.

(2) The local neighborhood inhomogeneity of the same window can be reflect by the pixel intensity relationship of that window and therefor adjusting different α values for different pixels can avoid the blur for the given image.

Finally the result of updating each of cluster centroids and membership functions were able to constrain the membership value of different classes to be negatively correlated at neighboring pixels.

In the experimental results the proposed algorithm was compared with other fuzzy c-mean algorithms such as: FCM_S, FCM_S, FCM_S2, and FLICM using synthetic and real MRI images. The validation was measured by using two validity functions: fuzzy partition and feature structure. After adding different types and levels of noise to synthetic and real images the results showed that the proposed algorithm achieved high and accurate performance in both clustering and segmentation results.

This proposed work is good for the advantages of being an unsupervised method that is fast and doesn't require any training information which is not available in some cases. The segmentation performance of the modified FCM method was good and achieved high results compared with other standard FCM methods due to the good way in which the FLICM algorithm was exploited by updating each of the cluster centroids and membership function. On the other hand Fuzzy c-Mean algorithm has some disadvantage such as the computational time needed for the convergence and also the fuzzy membership selection is not very easy. Another disadvantage was using fuzzy partition where partition coefficient and partition entropy measures the fuzzy partition and lacks the feature property direct connection.

2. Li-Hong Juang and Ming-Ni Wu, in [14] provide a color-converted segmentation method based on K-means clustering technique. This approach is used to segment the tumor partition from other MRI input objects. The main idea of this algorithm was converting the input MRI image in gray-level into a color space image and then separating the tumor from other objects in the image by using K-means clustering. The color converted image makes the segmentation process much easier where it helps to distinguish the tumor object from other brain components in the image. The K-means clustering method is used to partition the image data into k clusters based on the similarity and distance measures. K-means method is realized by assigning each data clusters to the nearest centroid which is then used to label new data clusters. The writers of this paper produced the K-means clustering method as following:

- a) Choosing the number of k clusters to be created.
- b) Segmenting the input data into k clusters by allocating each data point to its closest clustering centroid using a distance measure, for instance, Euclidean distance[15].
- c) Calculating the clustering matrix represented in the binary membership value of j to the cluster of i.
- d) Re-calculating K centroids.
- e) If the clustering centroids or matrix does not change then stop; otherwise go to Step 2.

A color-converted segmentation algorithm is used by the team of this paper. The method converts the colors of the image into a single integer index. This index is then used to pick out a color from a particular color list in a data collection which includes an R-G-B color format weighting vectors (L) and also a list from R colors. Mapping process is done in the following steps:

- a) The weighting vector L is first divided by its component summary for normalization.
- b) Calculating index $J = \text{round}((R - 1)(L1 \times C1 + L2 \times C2 + L3 \times C3) + 1)$, where C1, C2, C3 denotes red, green, blue respectively.
- c) Use the index J to pick out one of the inputs in the color list.
- d) This selected color needs to be classified more accurately by using a clustering method in order to separate the color objects in the image.

The final segmentation results shows that using the combination of color- converted segmentation with K-means achieves good results by separating tumor part from other brain components in the color image.

As a result, the proposed algorithm has some advantages where K-Means algorithm is computationally fast in comparison with other hierarchical clustering methods. It is also robust and easy to implement and very efficient in terms of using large collection of data. On the other hand if we want to discuss the disadvantages of this paper, the results of the proposed method showed that best results were given only from T2-weighted MRI sequence. However, giving good results depend on the original MRI image gray-level gradation. Another disadvantage is that the number of K clusters has to be specified from the beginning. Finally, in spite of achieving good results, we found that the proposed method needs more development for better accuracy specially in terms of using other MRI image modalities.

2.1.5 Classification Methods:

Classification techniques are important to classify the tumor region during its various stages. This technique requires precision because in some cases tumors boundaries could be difficult to detect and result in a false diagnosis. Therefore, to avoid such problems the help of computer is needed in order to obtain good accuracy results of determining and classifying tumors. Several classification techniques have been offered where the most common ones as Artificial Neural Network and Support Vector Machines are presented in this section as follows:

1. Ruan et al. [16]. The researchers of this paper have proposed a supervised machine learning system to track the tumor size during the treatment period. They propose a Support Vector Machine (SVM) classifier where four types of MRI images (T1, T2, PD, and FLAIR) were used in order to give complete information about the tumor region. A multi-scale scheme was performed in this study to reduce the processing time.

The scheme consists of two main steps, in the first step only T2 sequence is used to characterize the abnormal area by using the SVM classifier because it has a good visibility. The abnormal area is then extracted from all the sequences in the second step by performing SVM again to segment the tumor region.

The proposed segmentation system consists of 4 stages: registration, learning, SVM classification, and quantification. At first all slices of MRI data corresponding to the four MRI image types (T1, T2, PD, and FLAIR) are registered to the system. Learning stage is implemented in two phases, first only one slice of MRI data will be carried out manually (T2), and then other MRI types (T1, PD, and FLAIR) can be automatically learned. The classification stage consists of two steps: firstly, the slices are divided into small window sets and classified into two types' tumor and non-tumor. Where decreasing the images size leads also to decrease the consuming time of the method. Then the outcome of the windows is utilized by SVM classifier. Secondly, after separating tumor and non-tumor regions the SVM is applied this time only on the abnormal field (tumor region) to classify each voxel. The result of this step shows the tumor quite clearly in white color.

Last stage of the system is quantification which provides important information in order to assess the presented medical treatment. This work has some advantages represented in using a multi-scale scheme which has reduced the consuming time. Also due to the learning knowledge which was previously done in the first step of examination the patient does not need to go through this step again in the following examinations. The outcome of the segmentation method achieved high and accurate result compared with other multi-class classification algorithms. On the other hand, SVM classifier has some disadvantages, including the complexity of applying the algorithm where it requires a large amount of storage for classification and using other indirect techniques. Furthermore it is hard optimization and some classification errors may occur. The T1 sequence is used although to its poor contrast compared with other MRI sequences.

2. Kishore K. Reddy, et al, in their research [17] proposed a confidence surface to guide the enhanced brain tumor segmentation process using multi-parametric magnetic resonance imaging (MRI). They used the texture information for each of fluid attenuated inversion recovery (FLAIR), T1 weighted pre-contrast (T1pre), T1 weighted post-contrast (T1post), and T2 weighted (T2) MRI images as the inputs to train a discriminative model for detecting and segmenting the tumor. The framework of this work consists of four main sections: Extracted Texture Features of multi-parametric MRI images, Classification approach based SVM, AdaBoost classifier, Generating a Confidence Surface, and Implementation of Segmentation Methods. In the first section, researchers used each of Mean Intensity (MI), Histograms of Oriented Gradient (HOG), and Local Binary Pattern (LBP) features extracted from the spatial neighborhood pixels to deal with each of intensity, gradient, and variance information's respectively. These features were used by the team of this paper because of their successful and effectiveness use in many fields like faces recognition and object detection. Before extracting MI, HOG, and LBP features a mask is created in order to speed up the method process time. The mask was produced only for the enhanced tumor region by the difference of each T1pre and T1post images. After that, the mask is used to calculate the features of the enhanced regions for each of T1pre, T1post, FLAIR, and T2 images.

The extracted features in the first section was used to train a discriminative classifier by creating a feature vector and then this vector was given as an initial input to two classification methods which are SVM and AdaBoost to classify the tumor . These two classifiers are carried out by separating a set of data having different class. The classifiers are used to classify normal and abnormal cases where pixels are determined as tumor or non-tumor by the features extracted during the training stage. These pixels are then used to generate the target classes for testing the data. By using the same features for each detection method the True Positive Rate (TPR) and False Positive Rate (FPR) showed that AdaBoost was better than the SVM classifier in terms of the Receiver Operating Characteristic (ROC) curves. So AdaBoost was used in the rest of the method for tumor segmentation guidance. The third stage of this study was creating a confidence surface to guide the tumor segmentation. The classification output of the designed classifier is used to create a confidence surface.

Where the generated confidence surface contained noise, researchers used 2D Gaussian distribution in order to make the confidence surface smoother.

The last stage in this study was applying segmentation algorithms where the confidence surface was used as an initial guide to the segmentation process. Two classical segmentation techniques which are Level Set and Region Growing were used in order to achieve the segmentation accuracy. Confidence surface and T1 post MRI image are used as inputs for each of the modified segmentation methods. In the Level Set Model the object boundaries can be determined by evaluation which is done by the energy functional minimization. Researchers in this proposed method added a new energy functional in order to divide the confidence surface into two regions, tumor, and non-tumor. In Region Growing Method a neighbor pixel of a selected seed point $S(x, y)$ is checked whether the intensity of that neighbor is smaller than a threshold or not. If yes, the neighbor was added to the region to be grown and the mean intensity was recalculated iteratively until all seed point neighbors are checked. In this work region growing is used based on confidence surface to determine tumor pixels. The region was growing by the similarity measure of a pixel $S(x, y)$ according to the confidence surface which specifies the tumor pixel.

Dice Similarity Score (DSS) was applied in order to measure the accuracy of the segmentation methods where the results using confidence surface achieves better results than the original level set and region growing. Also the region growing method gave a better performance results (DSS average of region growing = **0.69**, standard deviations = ± 0.14) than the level set performance results.

This proposed method has some advantages such as providing a new approach that allows experts knowledge to be added into image segmentation by using a confidence surface, which result in an automatic brain tumor enhancement to aid the radiologists. It successfully utilizes the multi-parametric MRI texture information besides intensity information. Another advantage of this work was the segmentation results which proved that using the confidence surface on the two segmentation methods provide better results than the classical segmentation methods.

On the other hand the proposed method has some limitations, comparing the results of the proposed method with the ground truth shows that the proposed method has a

limited accuracy where some of the brain structures like blood vessels cannot be totally excluded.

In spite of the use of confidence surface the DSS results doesn't give a very high values because the enhancing tumor is usually not too big. Also in some cases, missing or adding any pixel in labeling results could cause inaccurate results and obtaining low values of DSS. Researchers of this paper were still able to apply their work on more segmentation methods in order to achieve more reliable segmentation results.

3. El-Sayed et al in [18] offered a computer aided detection (CAD) system based on segmentation and classification techniques to detect brain tumor using MRI images. This system was designed to help the diagnostic capabilities of doctors instead of spending a lot of time in order to get an accurate diagnosis. Their proposed method consists of four main stages: Acquisition and Preprocessing, ROI Segmentation, ROI's Features Extraction and Selection, and Classification. In the first stage the researchers applied median filter and high pass filter to remove any noise in the image and also to make the image background clean. This stage makes the coming stages more effective and provides better results by enhancing the images quality. The second stage is segmentation where a feedback pulse-coupled neural network (FPCNN) was used. This stage consists of three sections: Receptive Fields, Modulation Product, and Pulse Generation. The aim of this stage is modifying the input by replacing the feeding input via input stimulus and the output feedback. In the third stage discrete wavelet transform was used to extract the features of MRI images. By using DWT images are transformed from spatial to the frequency domain. DWT decompose the image into four main sub-images: Horizontal and vertical low pass (LL), Horizontal low pass and vertical high pass (LH), Horizontal high pass and vertical low pass(HL), Horizontal and vertical high pass(HH). Writers in their work used a three level decomposition to extract the features of the image where LL sub-image represent the approximation component and the LH, HL, HH sub-images represents the detailed components of the image. After that a principal component analysis (PCA) is performed to reduce the large number of interrelated variables of the features and get an efficient classification method. This step is done

by utilizing the largest eigenvectors of the correlation matrix to model a new ordered variable dataset and obtain a lower dimensional feature space.

Finally, a Back propagation neural network (BPNN) classification technique was performed where the inputs are classified by the selected features in the previous step into target classes of normal and abnormal samples. The network consists of input, output, and hidden layers and the artificial neurons weights are updated in a single layer generalized for feed-forward networks. Two signals were specified in this study according to the used network: First, function signals which are considered as the primary inputs of the network and propagate forward into the network until reaching the end as output signals of the network. Second, error signals which arise at the output neurons and propagate backward into the network.

In BPNN, the learning phase is ended when the error between the network output and required output is minimized and then the network is used for the testing phase achieving the principle of output error minimization.

According to the experimental results of this study and also comparing the method with other approaches, we found that successful and powerful results were obtained by achieving high and robust classification results. (Sensitivity=100%, Specificity=92%, and Accuracy= 99%).

4. In the paper of [19] Dipali M. Joshi et al. discussed a method of brain tumor detection based on neural network classification. A computer based system was utilized to detect the tumor in MRI images where Astrocytoma was the type of brain tumors used in this study. At first preprocessing was performed using histogram equalization (HE) in order to detect the edges of the tumor. HE is used to adjust the contrast of the image so that image abnormalities like tumor which usually appears dark will be better visible. The second stage of their method is Threshold Segmentation which was applied after the edges of the tumor were detected. An intensity threshold was selected to differentiate between tumor region and background. As a result a binary image was obtained where the tumor is represented by the gray level 1 and the background is represented by the gray level 0. The third stage in this method is Tumor Contrast Enhancement (CE). The enhancement was

done by applying a sharpening filter. This filter was used in order to increase the contrast of tumor region so the tumor can be more noticeable. After image enhancement morphological operations is done using each of dilation and filling operators to fill the broken gaps and close contours respectively. The next stage is Texture Feature Extraction where five Gray Level Co- occurrence Matrix (GLCM) features (ASM, Contrast, Entropy, IDM, and Dissimilarity) were used to recognize the normal and abnormal regions. Finally, the back-propagation artificial neural network algorithm is used to classify tumor cells. This network consists of 1 input layer, 1 or 2 hidden layers, and 1 output layer. In the training process input data is given to the Artificial Neural Network repeatedly and compared with the desired output where error is computed. The error is then re-propagated to the network to be used for weights adjustment where by the iterations error is reduced in order to obtain the desired output. After fixing the value of the adjustment weights the ANN's are ready to be used to category the unknown input images.

The results obtained using the proposed system showed how efficiently it was able to segment and detect the tumor from the image. Doctors confirmed the validity and accuracy of the segmentation results and their ability to identify the tumor region.

5. S.N. Deepa and B.A. Devi, in [20] proposed a classification based Artificial Neural Networks diagnosis system for tumor detection. They utilized each of Radial Basis Function Neural Network (RBFN) and Back Propagation Networks (BPN) to classify the brain images into normal or abnormal classes. The aim of this paper was not to compare the classification techniques but to learn and study the advantages and disadvantages of each method. The researchers in their study explained the design and mechanism of each classification method. BPN is defined as a feedback network containing an input, output, and one hidden layer that works on the function which is responsible of classifying tumor and non-tumor regions. In this network the connection is only between upper and lower layers where there is no connection between neurons in the same layer. These connections carry the weight of the network. The data is fed to the input layer and goes forward through the network layers until reaching the output. BPN network contain also a training set that represent some parameters modified by a reference dataset. This training set is then used in the back propagation of error producing the new data.

In feed forward stage the activation function of hidden nodes are computed and then compared with its target values in the error back propagation stage in order to define the error of that node. Then a factor is calculated to re-propagate the error to the previous layers which is used in the final stage with the activation function to update the weights. The other network which was used in this study is RBF network that contains only two layers. By entering the data as inputs the neuron of the hidden layer computes the Euclidean distance (distance between test case and central point). The kernel function of the RBF network is then implemented using spread and the result is turn into the output layer. The activation function of hidden layers is computed where the output depends on the radial distance. After weights are estimated the outcomes are scaled and summed in order to get the final output of the network. The Training stage of the RBF network contains: first, determining the centers of hidden nodes and their spreads and second, estimating the output weights according to the centers and spreads.

The writers of this paper presented their classification methodology which consists of pre-processing where they first applied a histogram equalization method and then the region was isolated from the image followed by the feature extraction step. The statistical feature set that was extracted and used in this study were: Energy, Correlation, Contrast, Entropy, and Homogeneity.

After preprocessing was done the two classification methods were performed and the same testing dataset were used in order to realize the same accuracy. The normal and abnormal classes were acquired and then the evaluation metrics were figured (training and testing performance) to obtain the classification efficiency using sensitivity, specificity and accuracy measurements. The final accuracy results that they achieved from their work were good. The RBFN classifier achieved a higher result with an accuracy of 85.71%, but this result compared with other neural network approaches is not good enough as the ones mentioned in [18].

The main advantages of ANN approaches over other classification techniques are:

- ANN is a nonlinear model which is simple to use and easy to understand. It presumes linear relationships between predictor variables which makes it compatible with real world.
- Neural Network models provide high predictive accuracy because it has the ability to detect most possible interactions which leads in reducing errors.
- The ANN models are robust and work well even if the training set contains some errors because of its parallel nature.
- ANN gives fast classification especially when using large dataset where the learned target function is evaluated very fast.
- Artificial neural networks offers a powerful tool in which a well-trained network can be considered as an expert in the area of information that has been given to be classified. This tool is used to help physician to diagnose and solve problems in medical images and also making decisions even in difficult medical cases.

On the other hand Artificial Neural Networks has some disadvantages as follows:

- In order to design a Neural Network training data is required.
- Large networks require high processing time, leading to more time to get results.
- Large neural network causes computation effort.

CHAPTER 3

PROPOSED METHOD

In this chapter, our proposed framework to detect and segment brain tumors in Magnetic Resonance Imaging is presented. The main purpose of this system is to determine the exact location of the tumor in the MRI images and then extract the tumor using image processing segmentation techniques. The medical definition of a brain tumor is represented in the abnormal growth of a group of cells within the brain which causes problems. These tumors can be categorized into two types as cancerous which is named (malignant) or non-cancerous which is named (benign). In order to distinguish between these infected cells and other healthy cells this system was designed. In the following section the basic concepts and stages of our proposed system are presented and discussed extensively.

3.1. Proposed System

In our research, we provide an automatic system to identify and extract brain tumors from MRI images. The system consists of four major stages. First, the preprocessing of the MRI image is done by mapping the image intensities to a standard scale. This step is very important for image analysis as it helps to get better results. Then the Haralick Texture Features are extracted from the preprocessed image after dividing the image into blocks. After that ANN classification is performed to classify tumor and non-tumor pixels and finally the region growing algorithm is utilized to segment the tumor area from MRI image. The details and full explanation of each stage are given in this section. The system is intended to aid radiologists in reading and diagnosing abnormalities in the field of medicine.

The flow chart diagram in the figure below (Figure 2) illustrates the steps of the method indicating the image processing techniques that are used to classify and separate the tumor from magnetic resonance images.

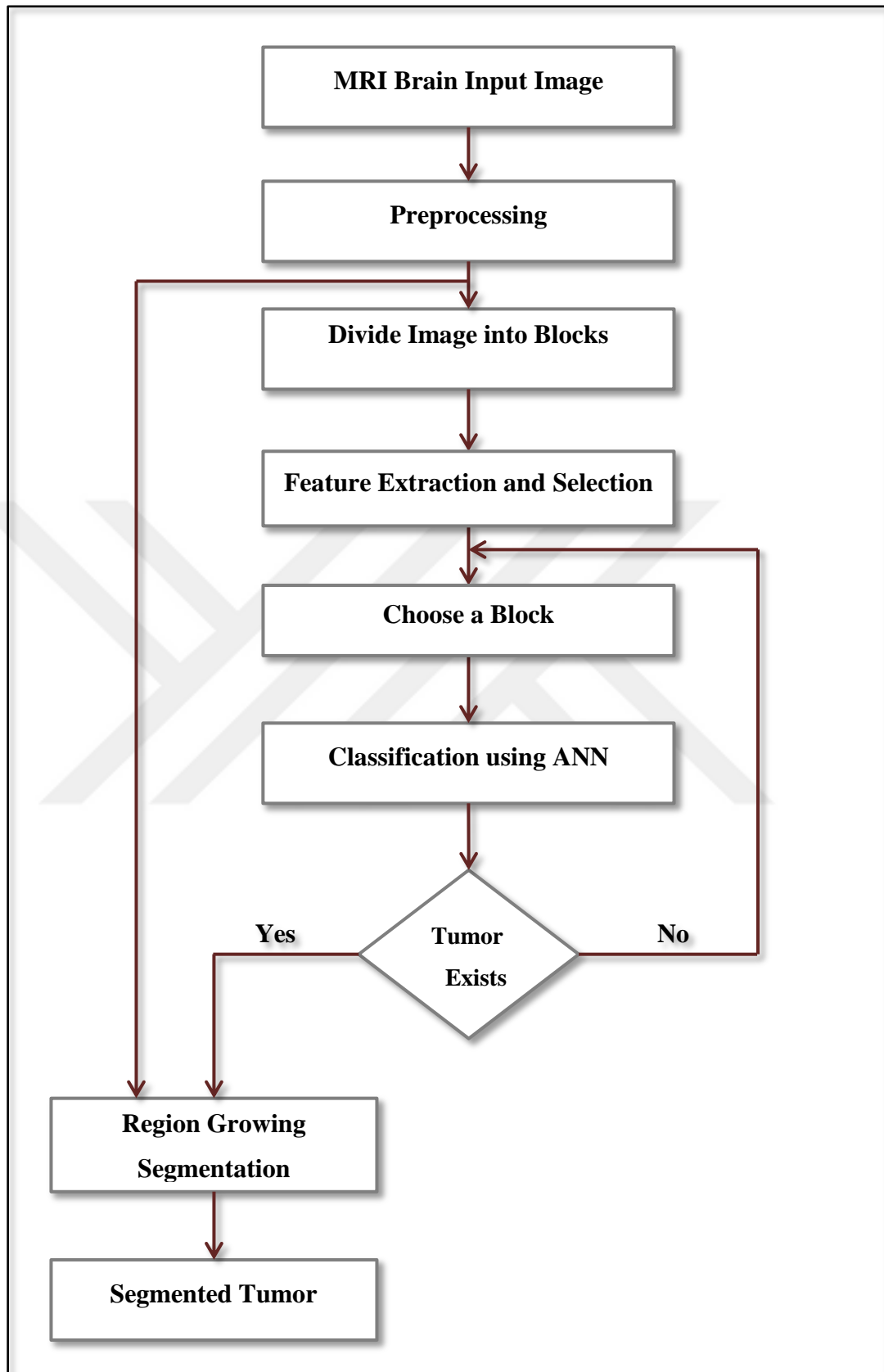


Figure 2: Flowchart Diagram of the Proposed Methodology

3.1.1. Preprocessing

In this step intensity normalization is performed by adjusting the pixel intensity range to a uniform grayscale. The main objective of this process is to increase the large dynamic range of MRI images to a standard range to be able to distinguish between different image tissues because the range of grayscale values varies from an image to another. This step plays an important role in terms of image analysis in order to obtain more accurate results. The sub steps of this stage are shown in the Figure below:

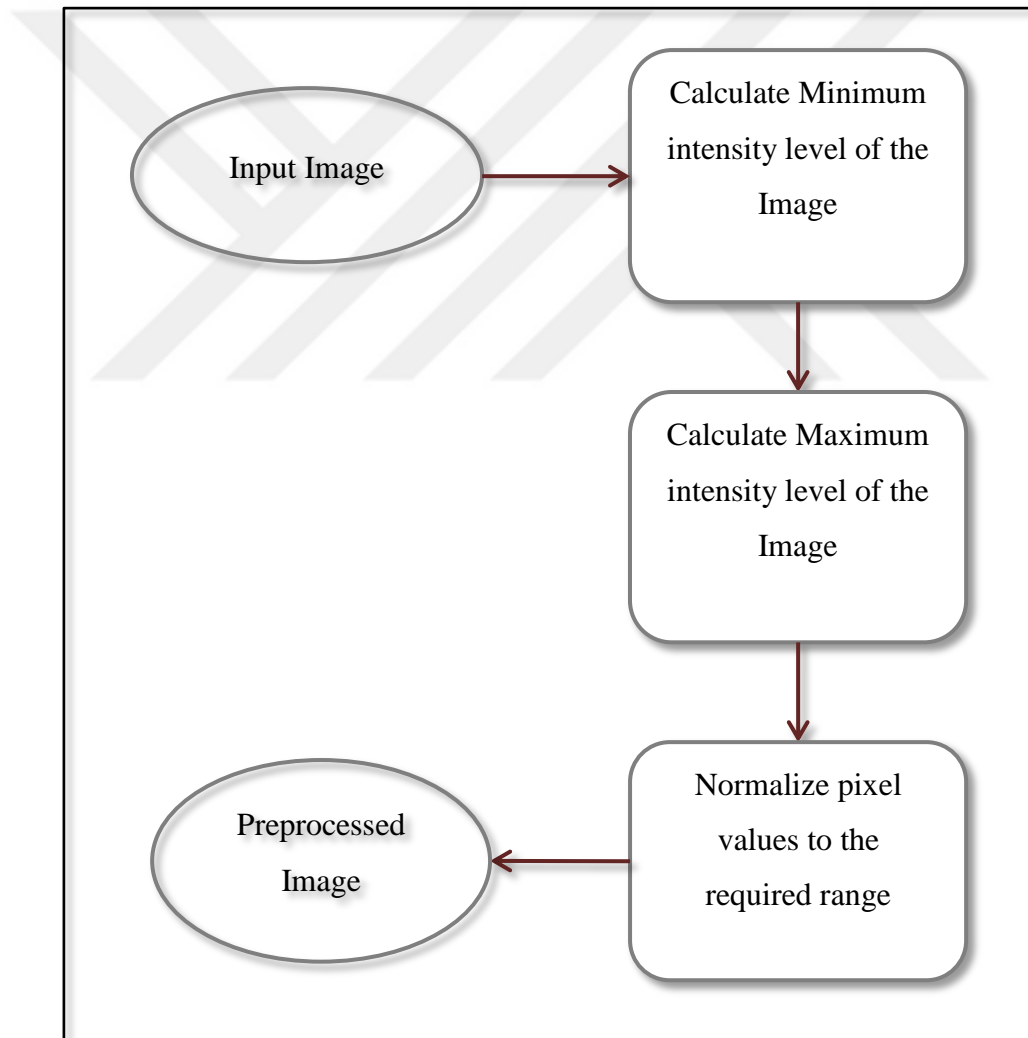


Figure 3: The Steps of Preprocessing Stage

The normalization process is described in the following points:

- First, calculating the minimum intensity level of the original image.
- Second, the maximum intensity level is calculated.
- Finally, the normalization is computed using each of values above.

The linear equation of grayscale MRI image normalization is given below:

$$f2(x, y) = ((f1(x, y) - f1min)/(f1 max - f1 min)) \quad (3.1)$$

Where: $f1(x, y)$ is the grayscale of the original image, $f1min$ and $f1 max$ represents the minimum and maximum grayscale values of the image, $f2(x, y)$ is the result of the normalization process. Figure 4 shows a snapshot of original image before and after the normalization using histogram.

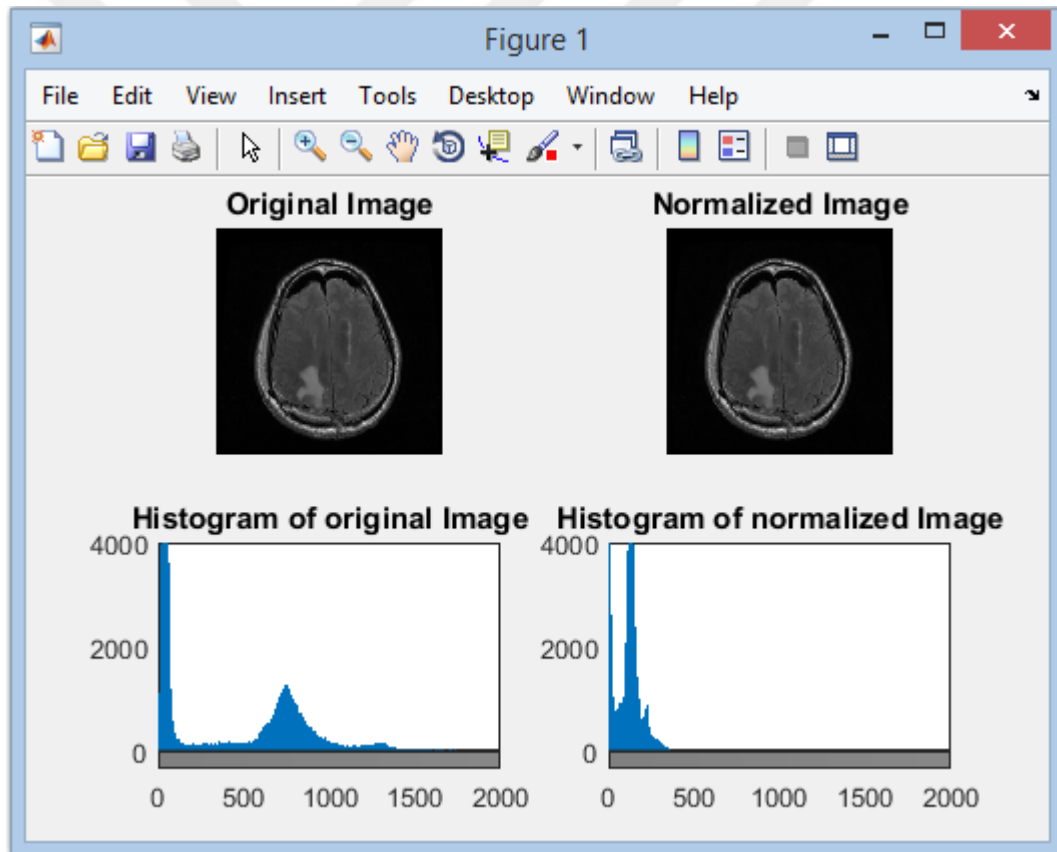


Figure 4: Histogram of Original and Normalized Image

3.1.2. Divide Image into Blocks:

In this work, After preprocessing step was performed the digital MRI image with (512×512) pixel size is divided into (8×8) blocks) which means 4096 sub images in order to first calculate the features of the blocks then these features are used as inputs to build the neural network.

3.1.3. Feature Extraction:

The feature extraction is one of the most effective and useful tools in the medical field that are used to distinguish and classify abnormalities in MRI images. The aim of these features is providing meaningful information to specify the characteristics of the area of interest by implementing statistical operations. In order to extract and select the features, the preprocessed image (512×512 pixel size) was first divided into 8×8 sub blocks and then the Mean of each block and the 13 texture features (Haralick Texture Features) for MRI images are calculated and extracted from both normal and abnormal blocks. Then the selection process of these features is done based on the ones who gave optimum results. Figure 5 presents the sub steps of the feature extraction stage.

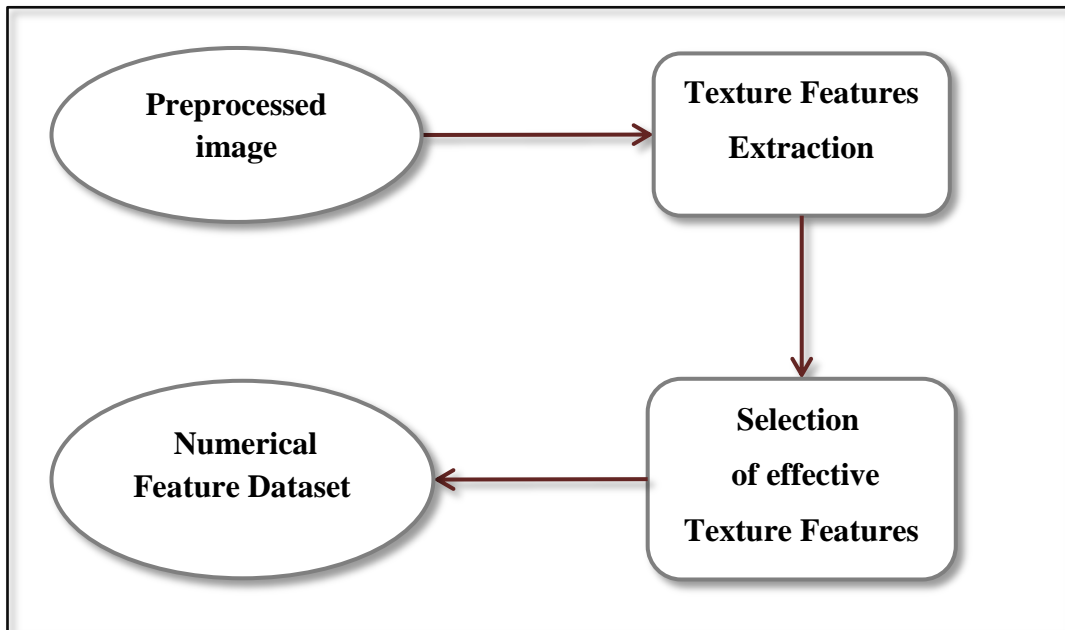


Figure 5: Block Diagram of Feature Extraction sub steps

Statistical features used in this stage are:

3.1.3.1. Mean of blocks:

In this step the mean which indicates the average of all pixels in a block was calculated. The equation used to calculate the mean is given as follows:

$$\mu_1 = \frac{1}{mn} \sum_{x=1}^m \sum_{y=1}^n g(i, j) \quad (3.2)$$

Where $m \times n$ indicates the size of block for the image $g(i, j)$ at (i, j) coordinates.

3.1.3.2. Haralick Texture Features:

13 Haralick texture features which were first use in 1973 [8] are calculated and extracted in this step in order to select the most effective ones in determining the characteristics of the tumor tissue using the Gray Level Co-Occurrence Matrix (GLCM) function. This function identifies the relationship of a pixel in a gray level image with its neighbor at different directions.

1. Mean: the mean in this step indicates the average of block pixels of the gray co-occurrence matrix. The calculation is done using the next formula:

$$E1 = \mu = \frac{1}{MN} \sum_{i=1}^M \sum_{j=1}^N p(i, j) \quad (3.3)$$

Where, $M \times N$ is the size of image and $p(i, j)$ represents the probability of the co-occurrence matrix at (i, j) coordinates.

2. Standard Deviation: the standard deviation measures the dispersion of the pixels around the mean at selected distance in the GLCM. it can be obtained by using the following formula:

$$E2 = \sqrt{\frac{1}{MN} \sum_{i=0}^M \sum_{j=0}^N (p(i, j) - \mu)^2} \quad (3.4)$$

- 3. Contrast:** This feature returns the local intensity difference of the gray-level co-occurrence matrix.

$$E3 = \sum_{i=1}^G \sum_{j=1}^G |i - j|^2 p(i, j) \quad (3.5)$$

Where, G indicates the number of gray levels utilized in the co-occurrence matrix.

- 4. Correlation:** indicates the pixel gray level linear dependence to its neighbor in the co-occurrence matrix.

$$E4 = \sum_{i=1}^G \sum_{j=1}^G \frac{(i-\mu_i)(j-\mu_j)p(i, j)}{\sigma_i \sigma_j} \quad (3.6)$$

Where μ_x , μ_y , σ_x and σ_y indicates the means and standard deviations of the probability function of co-occurrence matrix $P(i, j)$.

- 5. Energy:** it calculates the sum of uniformity of the gray levels pixels in the GLCM. In this case, the uniformity value will be large if the pixels are very similar.

$$E5 = \sum_{i=1}^G \sum_{j=1}^G (p(i, j))^2 \quad (3.7)$$

- 6. Homogeneity:**

$$E6 = \sum_{i=1}^G \sum_{j=1}^G \frac{p(i, j)}{1+|i-j|} \quad (3.8)$$

- 7. Entropy:** this feature returns a value that measures the degree of randomness which describes the texture in the image. The following equation is used to calculate entropy value:

$$E7 = - \sum_{i=1}^G \sum_{j=1}^G p(i, j) \log(P(i, j)) \quad (3.9)$$

- 8. Root Mean Square:** is used to estimate the root mean value of the co-occurrence Matrix (GLCM). The RMS is given in the equation below:

$$E8 = \sqrt{\frac{\sum_{i=0}^M \sum_{j=0}^N (p(i, j))^2}{M \times N}} \quad (3.10)$$

9. Variance: This feature depends on the average so that weights are used to distinguish between elements that differ from the average.

$$E9 = \sum_{i=1}^G \sum_{j=1}^G (i - \mu)^2 p(i, j) \quad (3.11)$$

10. Smoothness: is used to measure the gray level contrast in the GLCM in order to set the descriptors of other relative smoothness.

$$E10 = 1 - \frac{1}{1 + \sigma^2} \quad (3.12)$$

11. Skewness: this feature estimates the asymmetry of probability distribution that is relative to the mean value.

$$E11 = \frac{1}{MN} \sum_{i=1}^M \sum_{j=1}^N \left(\frac{p(i, j) - \mu}{\sigma} \right)^3 \quad (3.13)$$

12. Kurtosis: measures the number of peaks and flatness of the distribution and can be calculated as:

$$E12 = \left[\frac{1}{MN} \sum_{i=1}^M \sum_{j=1}^N \left(\frac{p(i, j) - \mu}{\sigma} \right)^4 \right] - 3 \quad (3.14)$$

13. Inverse Difference Moment: IDM is affected by the homogeneity where it provides a low result for inhomogeneous images, and a higher relative result for homogeneous images due to the weighting factor $(1 + (i - j)^2)^{-1}$.

$$E13 = \sum_{i, j=0}^{G-1} \frac{p(i, j)}{1 + (i - j)^2} \quad (3.15)$$

3.1.4. Feature Selection:

In this step, after calculating all features a number of blocks have been chosen automatically from both normal and abnormal regions to figure out which of their features was able to distinguish between suspicious and normal regions better than others. As a result 5 texture features have been chosen manually in this process due to the proximity of the texture results where (μ_1) was the better performance.

Five selected features of this stage were:

1. Mean (μ_1).
2. Contrast.
3. Variance.
4. Kurtosis.
5. Skewness.

3.1.5. Classification:

A neural network classifier is designed and proposed using Matlab in this stage. The aim of this technique is to identify and classify the suspicious abnormal tissues in the digital MRI images in order to choose a seed point for region growing method from those abnormal regions to segment the tumor. Figure (6) illustrates the structure of neural network. This stage is divided into two main steps: Training Process and Testing Process. In training process candidate features of 12 MRI images, which have been already chosen automatically from both tumor and non-tumor areas, were utilized to build the network. To create the network two sets of data elements are required. These two datasets are represented by two sample matrix of input and target vectors (candidate feature dataset as inputs and class attribute as targets). The inputs and targets are fed to the network in order to get the weights.

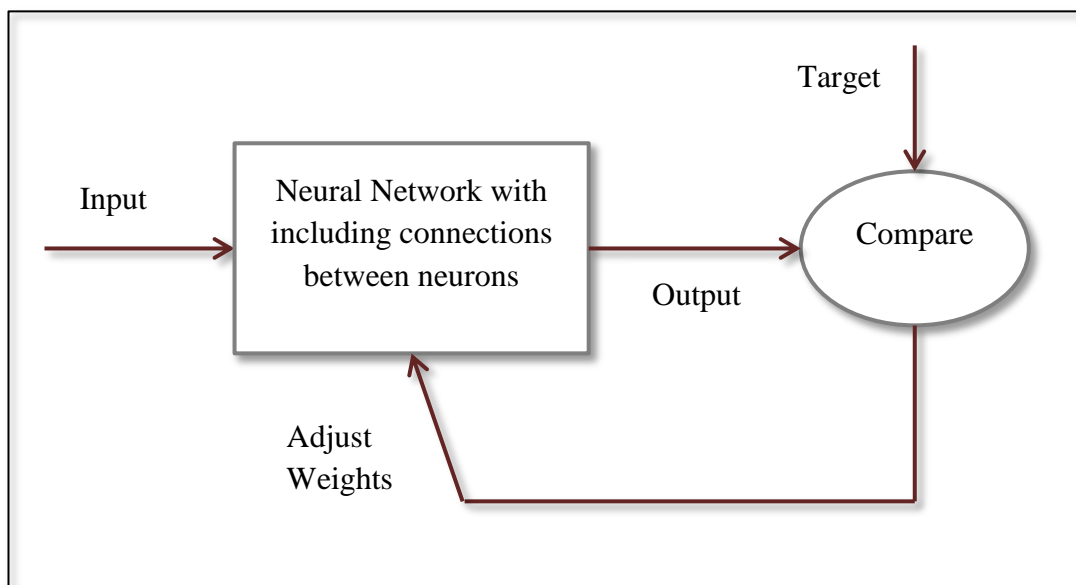


Figure 6: The Structure of the Neural Network

The proposed designed network in our study includes 25 input neurons and one output neuron. The following Figures indicate the ROC and Confusion Matrix of the training stage. In Figure (7) the ROC plot shows the success rate of the training phase which is 100% and the error rate which is 0% for all the actions in this stage. While in Figure (8) the Confusion Matrices of each action (training, validation and testing) is presented including the number of used MRI images for each one and also with a zero error rate. (Total number of used MRI images in this stage is 12). Finally Figure (9) shows the best validation performance of the training stage.

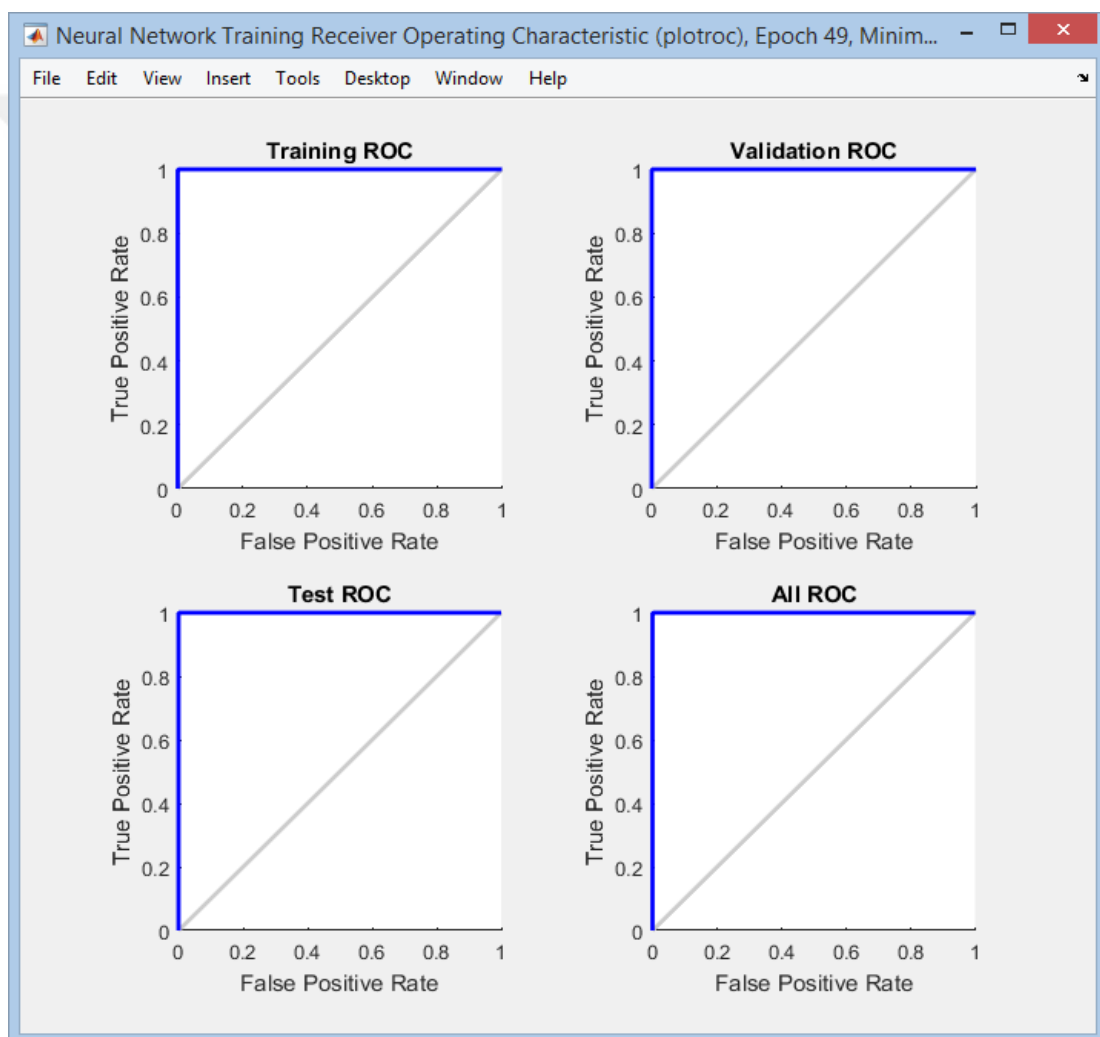


Figure 7: Snapshot of ROC in the Training Stage

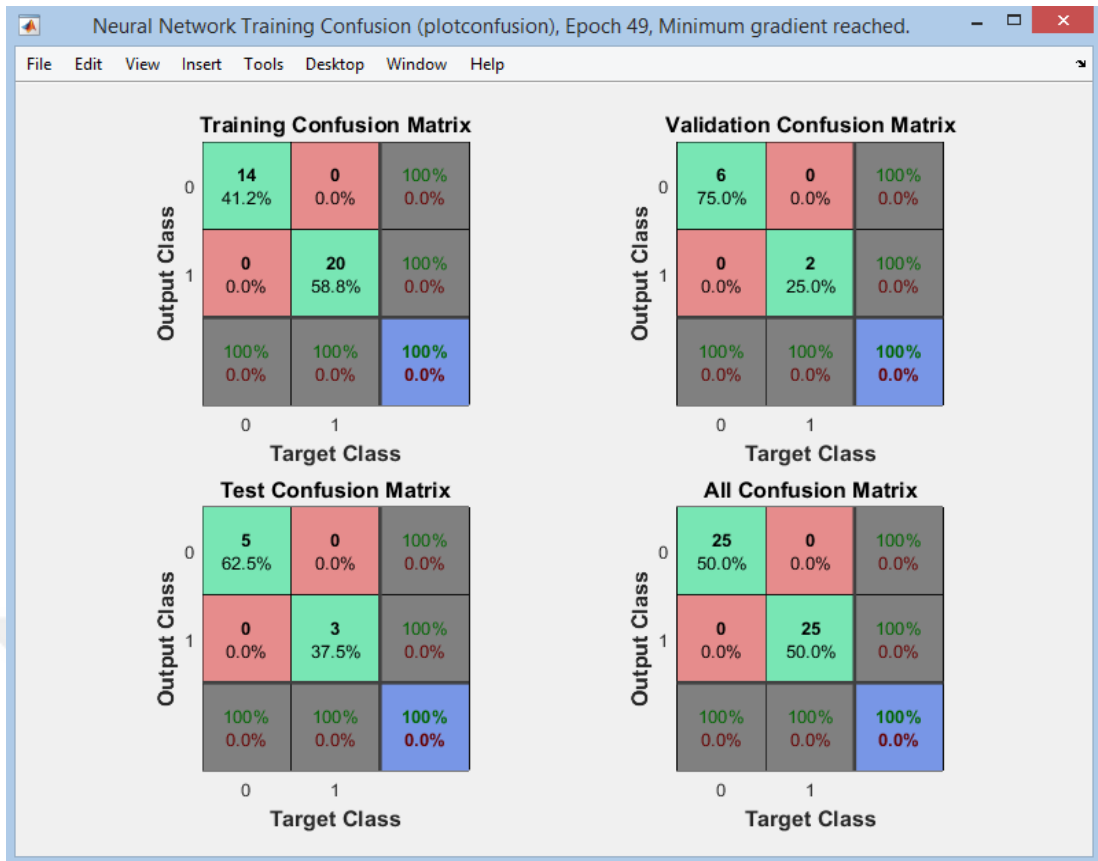


Figure 8: Snapshot of Confusion Matrix in the Training Stage

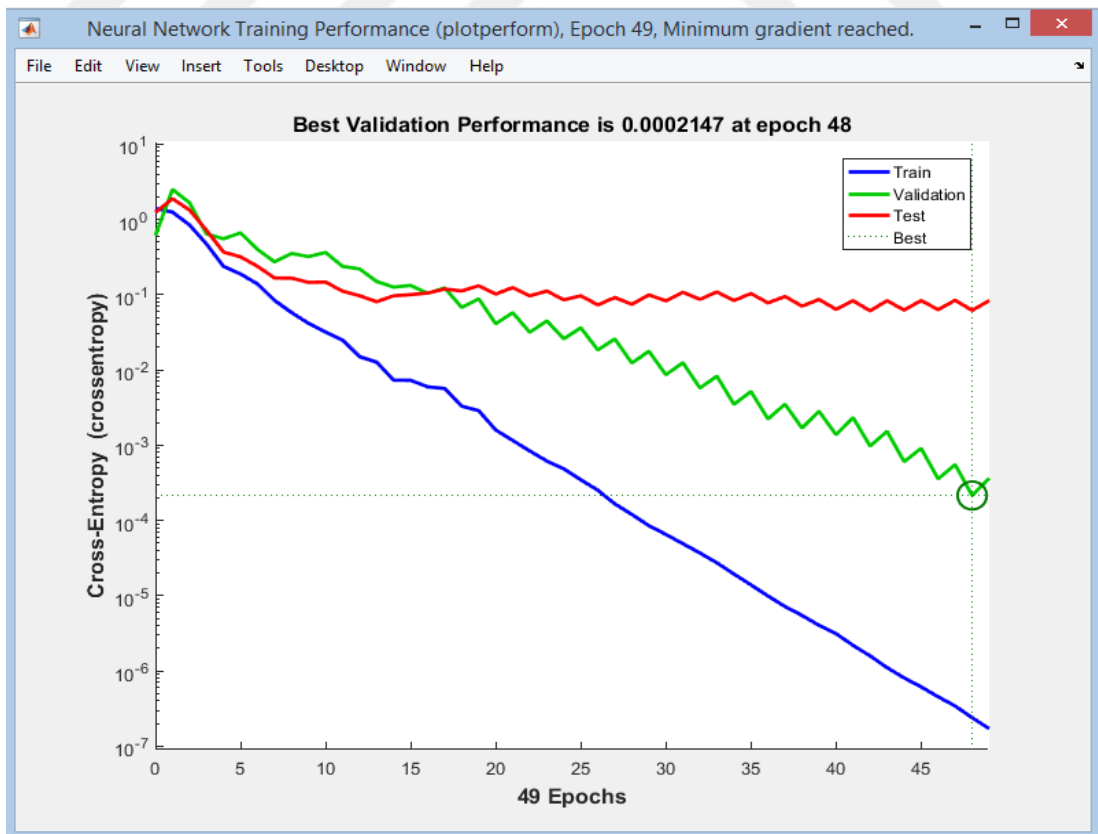


Figure 9: Snapshot of Performance in the Training Stage

3.1.6. Seed Based Region Growing Algorithm (SBRG):

Region growing segmentation method is considered as one of the region based techniques that depends on similarity and homogeneity in separating different objects of the image and provides precise tumor detection. The main objective of this method is to segment the Region of Interest (ROI) from the MRI image by selecting a specific point from the region to be segmented called "seed point" and then check whether the adjacent pixels have the same characteristics of the seed and therefore merge these pixels to the seed region. These similar pixels are merged iteratively together until the boundary of the region is determined. In this work, a seeded region growing method is used to separate the tumor area from the medical image while the seed points used are pre-identified at the previous step (Neural Network Classification). Figure (10) illustrates how the region growing algorithm works.

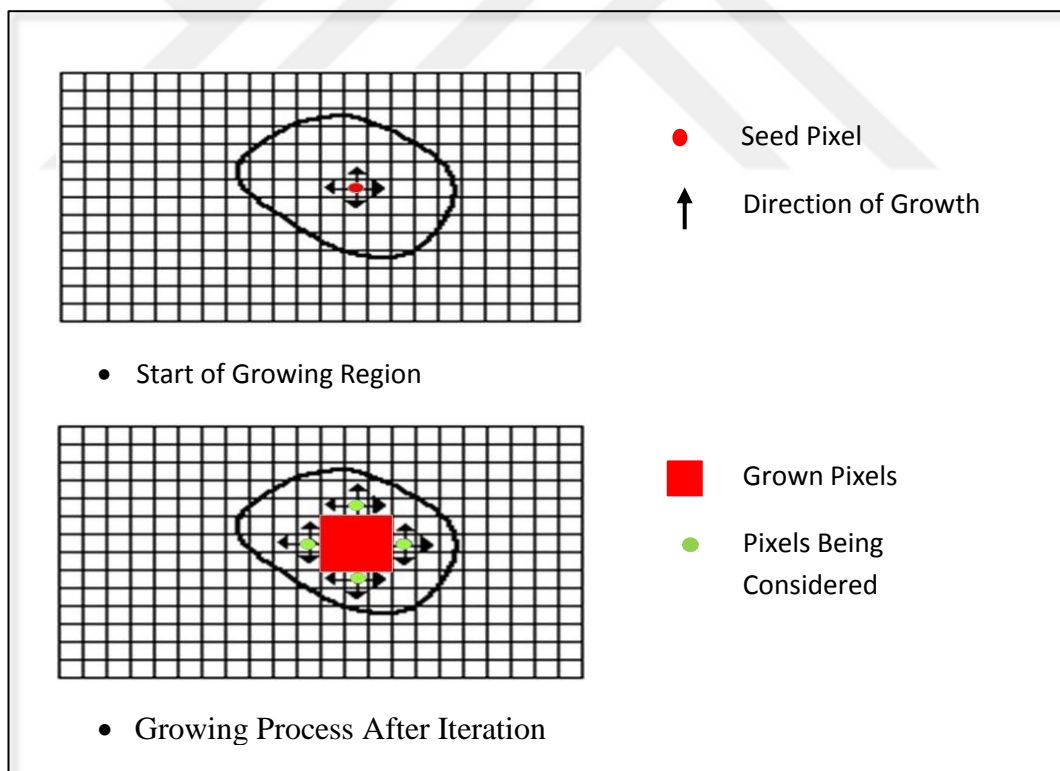


Figure 10: Region Growing Process

CHAPTER 4

EXPERIMENTAL RESULTS

In this chapter, results of proposed system detection methods using magnetic resonance imaging and the used tools are presented.

4.1. Data Source and Used Tools:

The brain magnetic resonance imaging dataset used in this thesis is The Cancer Imaging Archive (TCIA) which was produced and primarily hosted by Washington University in Saint Louis (<http://www.cancerimagingarchive.net/>) [19]. This database contains a large set of image data for different types of cancer disease, including brain cancer. The main file format used by the TCIA dataset is the Digital Imaging and Communications in Medicine (DICOM) format. The type of MRI images used in this study used is T2-weighted (T2WI) MR brain images in axial plane and with 512×512 pixel size.

Moreover, the magnetic resonance images included in this dataset provides some information about the patient such as the patient's gender, age and date of study.

The proposed automatic system in this study was built by using MATLAB® R2016b and a PC with the following specifications:

- Microsoft Windows 8.1 Pro © 2013 Corporation
- Intel(R) Core(TM) i7-4510U CPU @ 2.00 GHz 2.60 GHz
- 8.00 GB RAM
- 64-bit Operating System, x64-based processor
- Hard Disk Drive 1 TB

4.2. Proposed Method Experiments:

4.2.1. Preprocessing:

In this section, normalization was applied by modifying the range of pixel intensity to a standard range in order to decrease the dynamic range of MRI images. The result of grayscale normalization for 3 MRI images (000005-IM, 000001-IM, and 000025-IM) using histogram is presented in the following Figures:

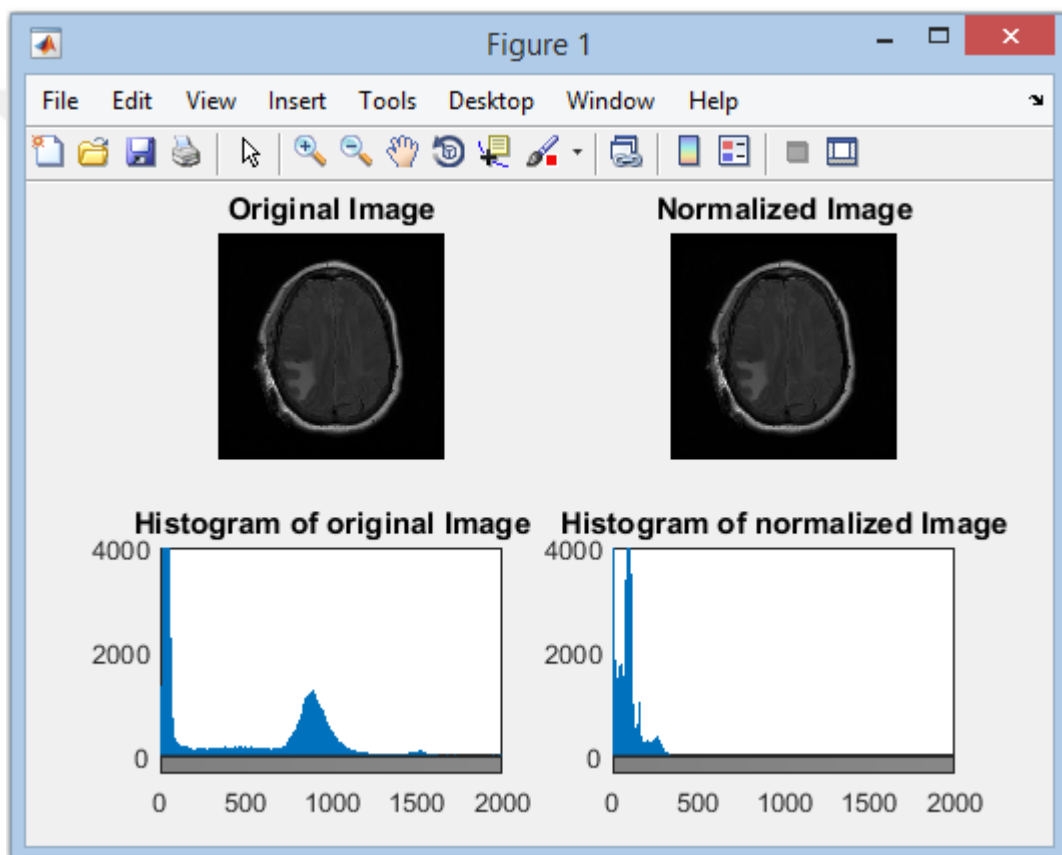


Figure 11: Snapshot Shows Histogram of 00005-IM Original and Normalized Image

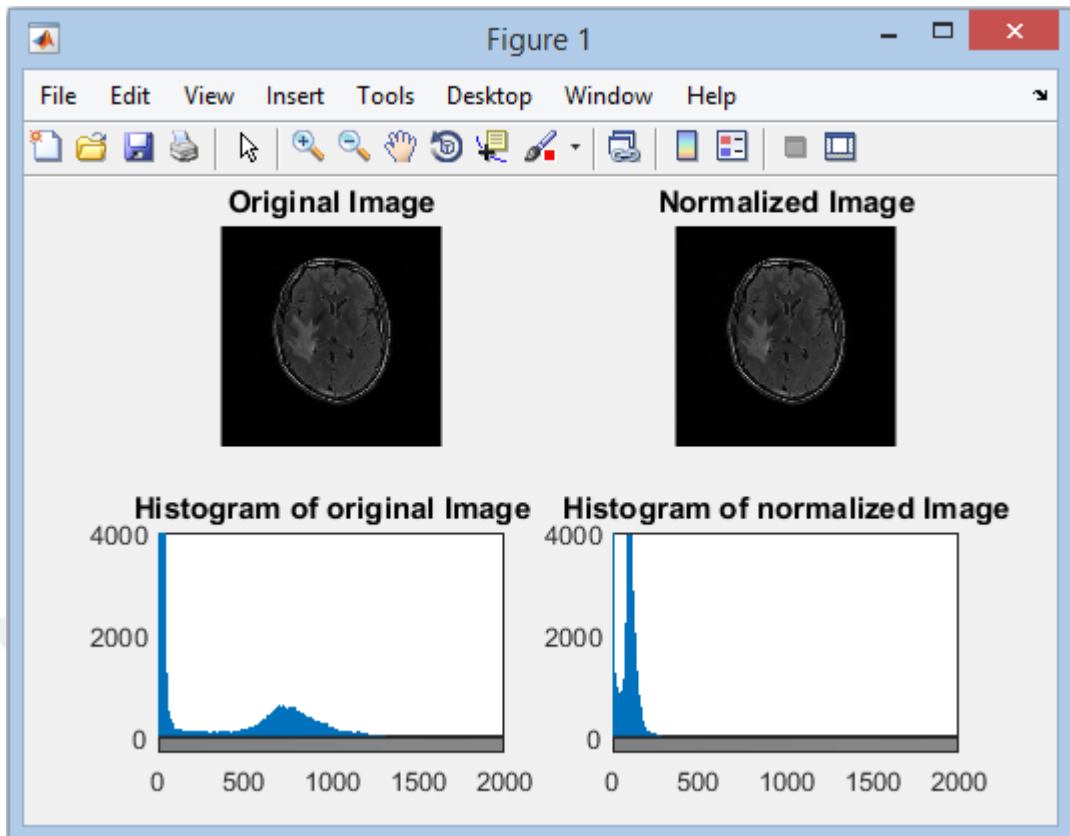


Figure 12: Snapshot Shows Histogram of **00001-IM** Original and Normalized Image

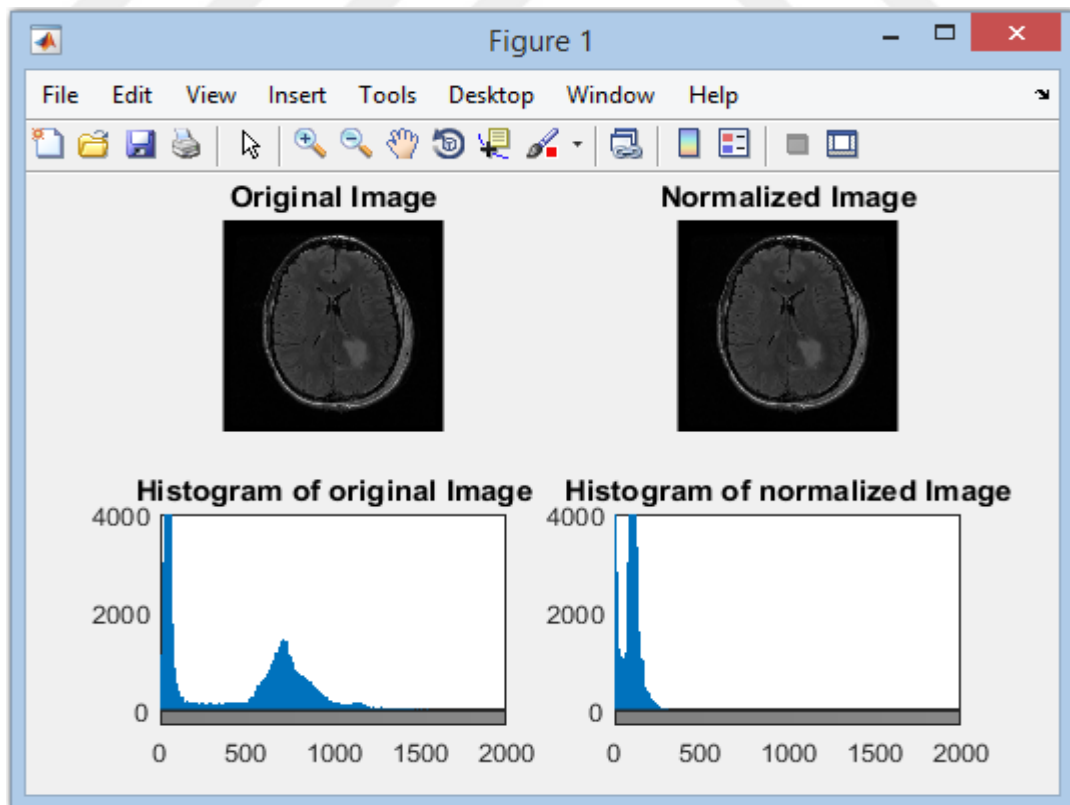


Figure 13: Snapshot Shows Histogram of **00025-IM** Original and Normalized Image

4.2.2. Dividing Images into Blocks:

In this section, the 12 digital MRI images with (512×512) pixel size were divided into (8×8) blocks which means (64×64) row-and-column blocks) while the total number of sub images was 4096. This process is considered as a preparation for the next step which is extracting the Haralick texture features for these blocks in order to utilize them after that in classification stage. Coming Figure display the divided image.

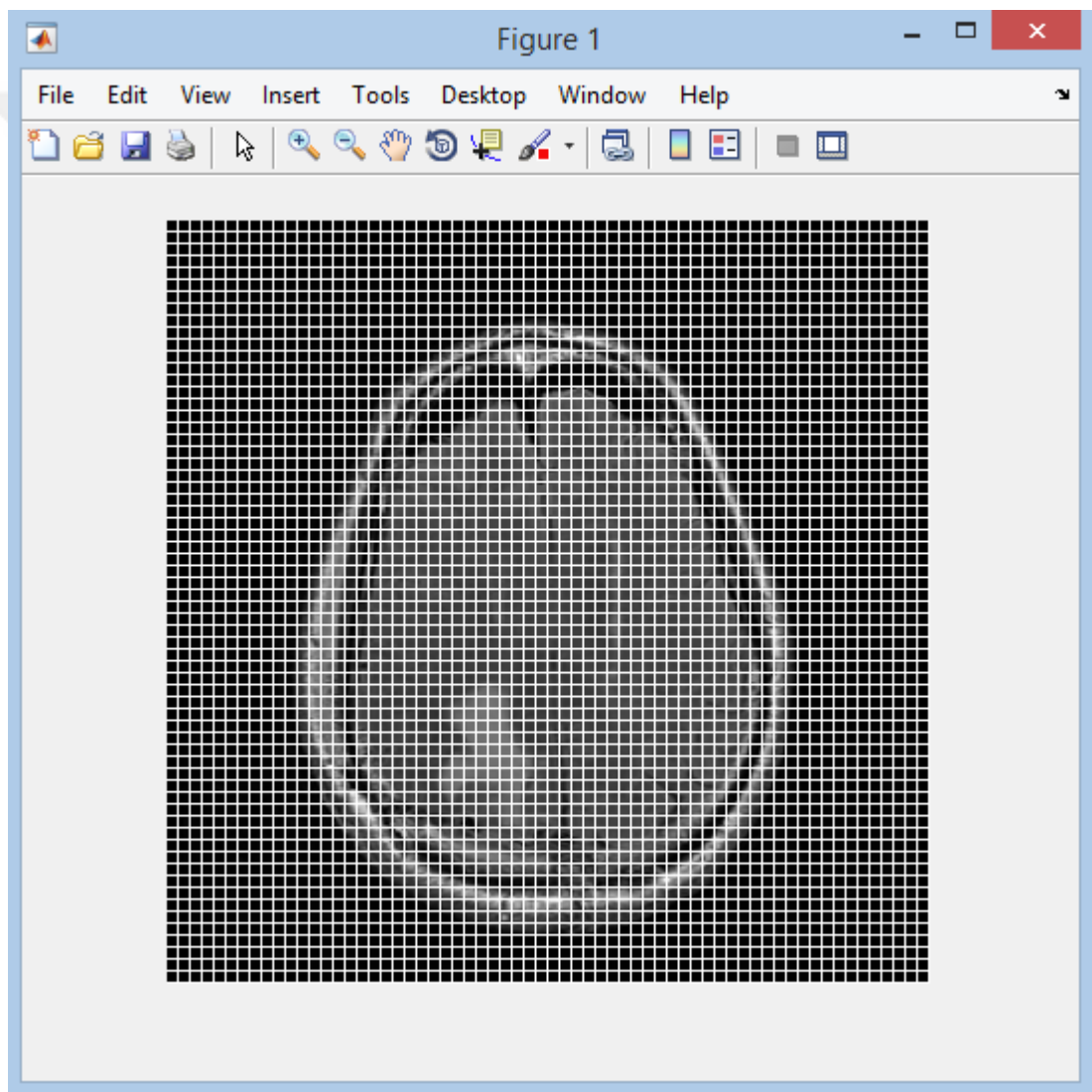


Figure 14: Snapshot of Divided the Image

4.2.3. Extracted Features:

Textures features calculation was done in this stage and the feature dataset was obtained. This dataset includes the extracted features of the five ones that have been selected in the previous chapter. A sample of extracted features and their class attributes which are indicated by the values (0 for normal tissues and 1 for abnormal tissues) are given in Table 1 below:

Table 1: Part of the Selected Feature Extraction Results and their Class Attributes

No.	Mean1	Contrast	Variance	Kurtosis	Skewness	Class Attribute
1	210.17	37.304	0.03242	77.501	7.7923	1
2	229.41	180.21	0.079923	168.26	12.272	1
3	162.45	142.86	0.21586	623.48	23.39	1
4	0.03125	70.875	2.8483	4089.8	63.928	0
5	10.953	67.143	0.061709	336.66	15.408	0
6	2.3906	118.13	0.56217	1509	37.063	0
7	17.531	140.79	0.044317	97.12	9.1777	0
8	209.83	58.036	0.032374	61.599	7.3024	1
9	180.3	59.964	0.04155	125.03	9.8274	1
10	207.09	83.75	0.057268	355.77	15.245	1
11	210.5	85.839	0.047495	218.42	12.337	1
12	222.48	63.643	0.086271	217.02	13.743	1
13	157.41	63.679	0.067716	204.3	12.777	1
14	0	0	3.0625	4094	63.977	0
15	6.3906	124.39	0.14899	390.58	18.73	0
16	94.969	77.464	0.037055	81.722	8.3024	0
17	3.5469	259.88	0.45234	1226	32.922	0
18	7.2813	109.59	0.1033	550.93	19.945	0
19	84.234	98.554	0.041473	115.79	9.5011	0
20	32.016	50.964	0.04169	131.14	10.154	0
21	189.59	101.8	0.0471	216.03	12.337	1
22	203.45	77.589	0.035544	111.41	9.0033	1
23	210.38	134.82	0.031808	98.702	8.2262	1
24	27.063	88.143	0.032048	77.501	7.7923	0
25	107.11	187.25	0.07904	170.45	12.371	0

4.2.4. Classification:

After the neural network was built and trained using the feature extraction dataset then the 12 MRI images are classified using the trained classifier in the previous chapter. The blocks of each divided image are tested by the network and those blocks which contain the tumor tissue will be classified as cancerous regions carrying the value 1 unlike, other normal regions carrying the value zero. As a result, all the tumors in the MRI images are classified and accordingly a seed point is selected within this area. The following Figure (15) displays a part of MRI image containing the tumor area and Table (2) shows the result of the same image after classification indicating the suspicious region (True Positive) in red in color.

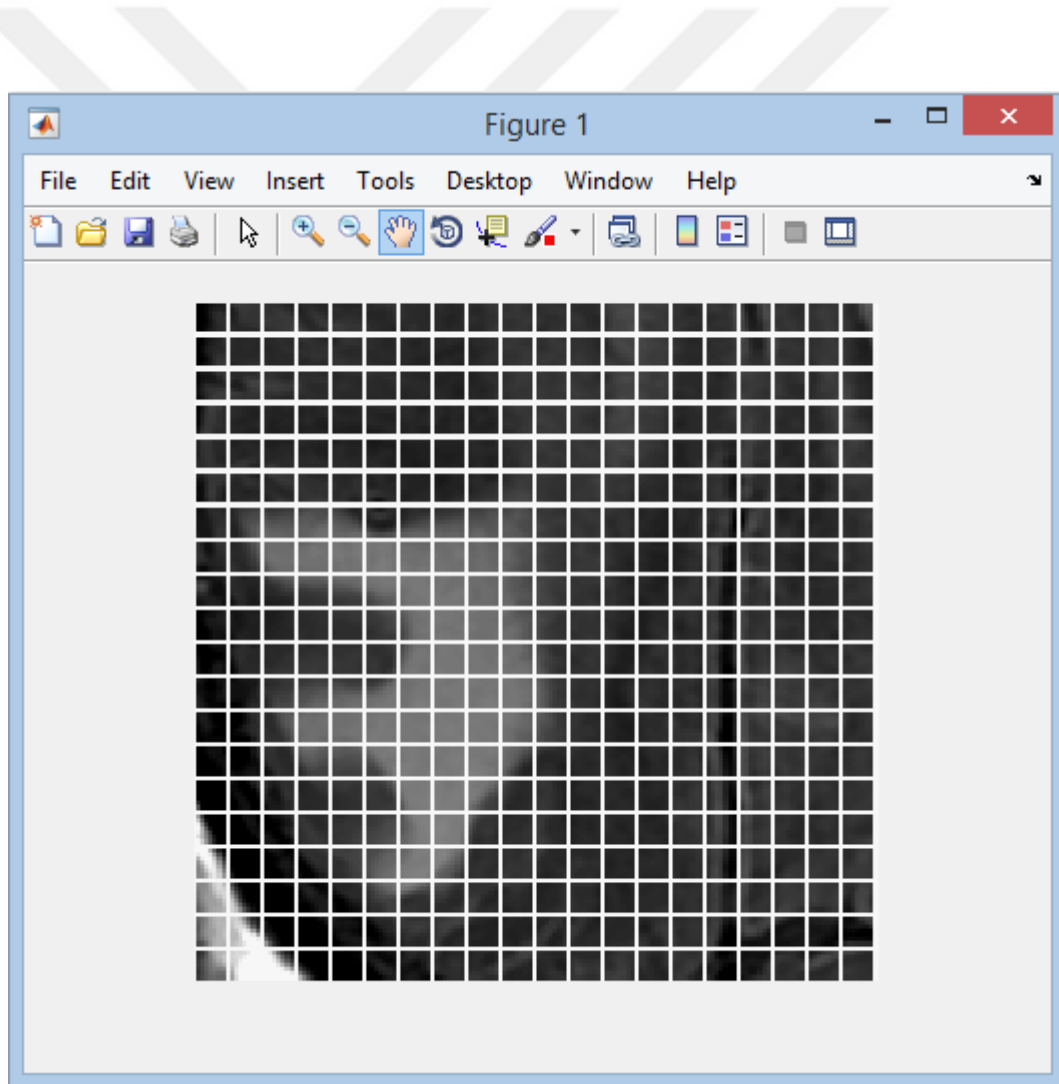


Figure 15: Snapshot of MRI Image (000005-IM) Showing Tumor Position

Table 2: Shows Part of Classification Result for (000005-IM) Image

	1	2	3	4	5	6	7	8	9	10
1	9.29E-09	1.36E-08	1.22E-08	1.05E-08	5.34E-08	1.26E-08	2.67E-08	1.91E-08	1.34E-08	3.29E-08
2	1.19E-08	9.03E-09	1.47E-08	1.01E-08	9.49E-09	1.19E-08	2.32E-08	1.97E-08	1.51E-08	2.72E-08
3	1.20E-08	1.56E-08	6.49E-07	9.81E-09	8.76E-09	1.22E-07	7.34E-09	9.42E-09	1.51E-08	1.83E-08
4	1.46E-08	1	1	7.65E-07	2.27E-08	0.09143	9.43E-06	3.84E-06	1.35E-07	1.95E-08
5	1.20E-08	1	1	1	1	1	1	1	1	1.91E-08
6	1.35E-08	2.57E-09	5.10E-07	0.00802	1	1	1	1	1	2.12E-08
7	8.87E-09	4.18E-10	1.00E+00	1	1	1	1	1	1	1.72E-08
8	1.45E-08	2.15E-09	2.71E-08	1.94E-08	6.39E-10	1	1	1	1	1.65E-08
9	5.89E-09	1.61E-09	0.00013	1	1	1	1	1	1	4.24E-08
10	5.85E-09	3.62E-10	1	1	1	1	1	1	1	2.25E-08
11	6.13E-09	4.81E-10	3.22E-08	0.98636	1	1	1	1	1.32E-07	6.01E-08
12	7.27E-09	3.42E-10	9.01E-10	2.78E-09	0.8588	1	1	1	1.44E-09	1.71E-08
13	6.01E-09	1.77E-10	5.26E-10	8.95E-09	2.34E-08	1	1	8.74E-09	5.39E-10	1.97E-08
14	4.50E-09	1.68E-10	2.39E-10	1.61E-09	1	1	1	5.23E-10	3.85E-10	1.39E-08
15	1.87E-08	4.09E-09	5.74E-09	6.81E-09	2.58E-08	0.0002	1.27E-08	1.94E-08	8.91E-09	6.57E-08

As can be seen in Table 2 the results of the neural network classification process achieved good performance and the seed point could be chosen from these true positive regions (TP).

4.2.5. Segmentation(Seeded Region Growing Algorithm):

Finally the segmentation process was done to segment the tumor area from the MRI image after selecting one of the seed points obtained from the classification results. The coming Figures (16, 17, 18, 19, 20 and 21) display the result of applying the region growing method on six samples of MRI images.

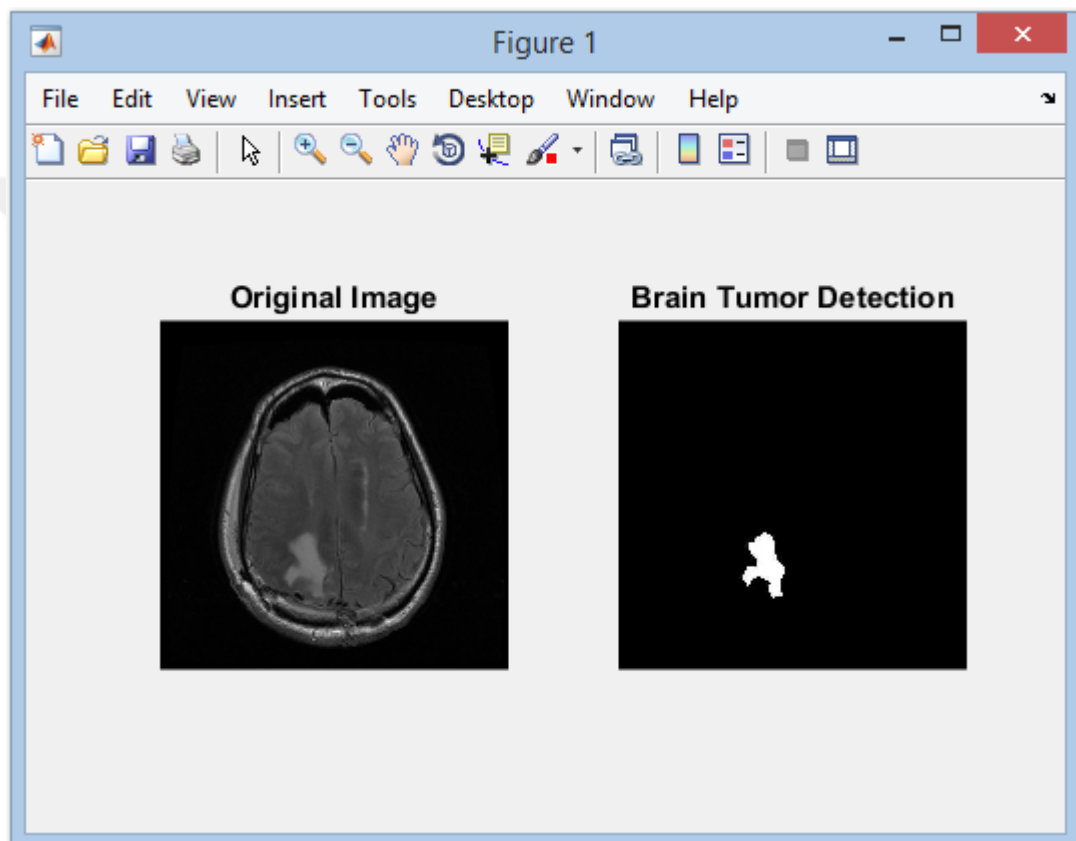


Figure 16: Snapshot Shows the Result of (000018-IM) After SBRG

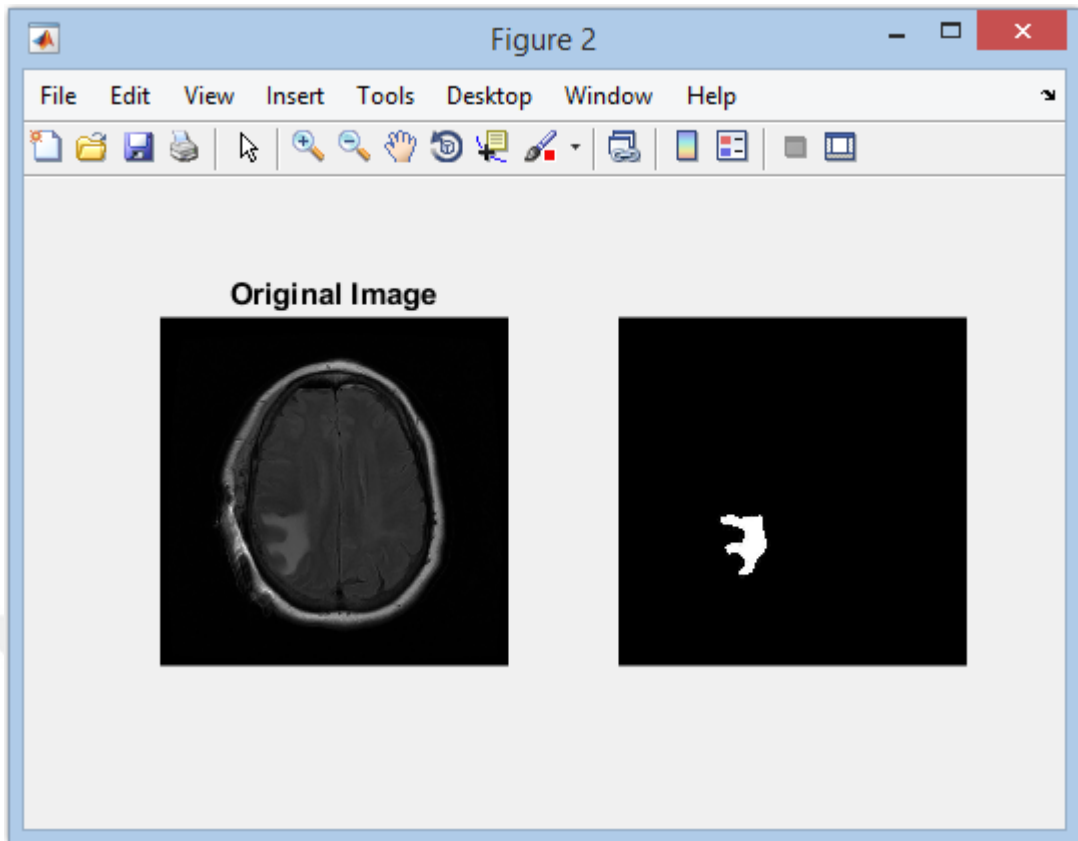


Figure 17: Snapshot Shows the Result of (000005-IM) After SBRG

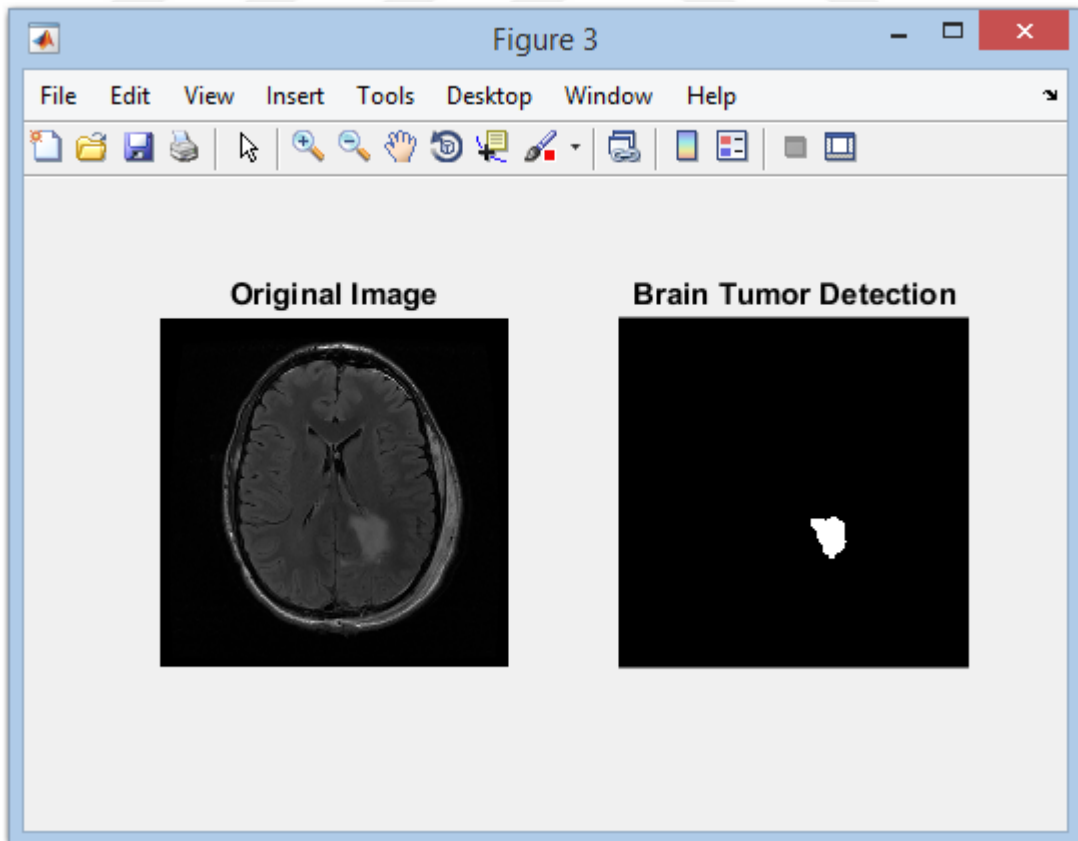


Figure 18: Snapshot Shows the Result of (000025-IM) After SBRG

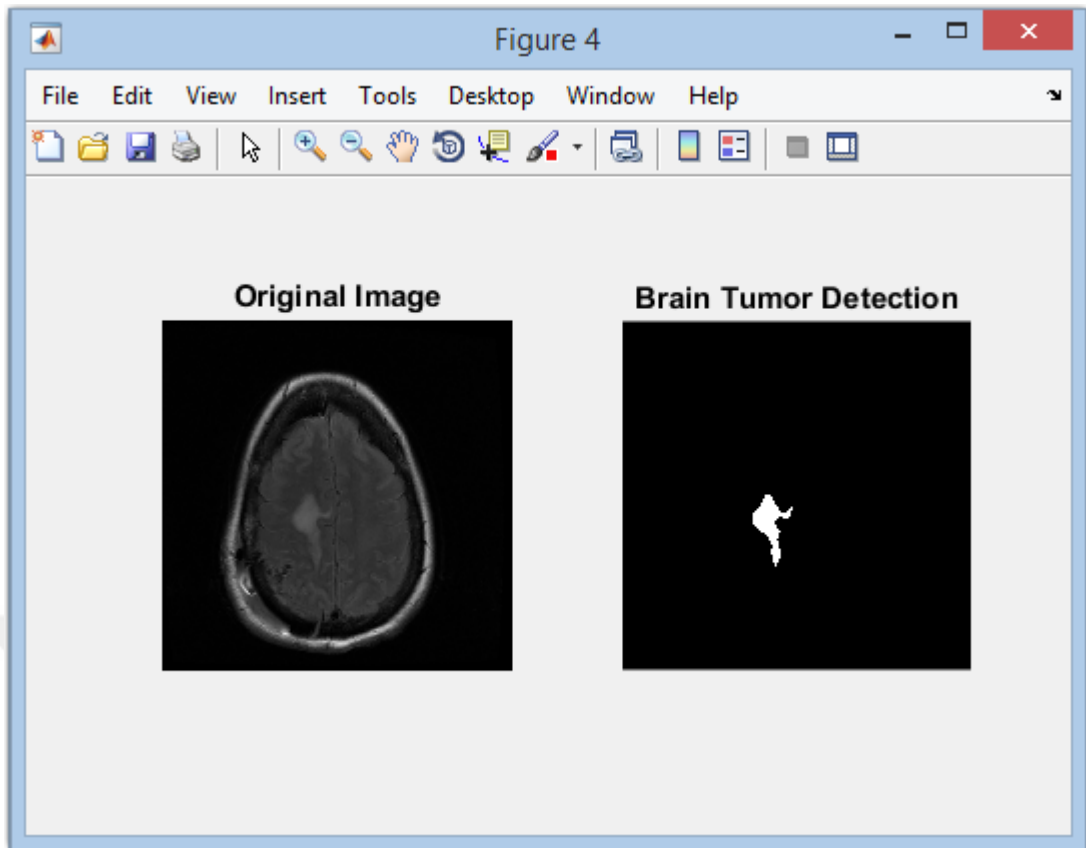


Figure 19: Snapshot Shows the Result of (000014-IM) After SBRG

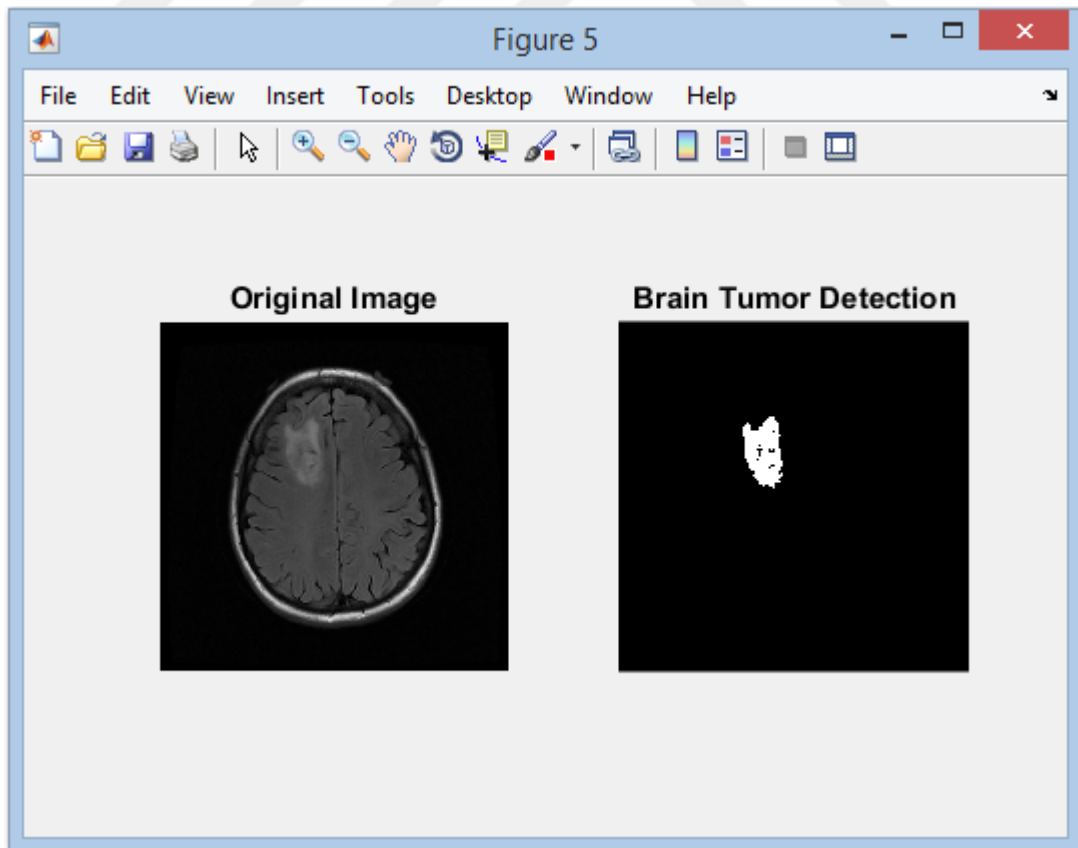


Figure 20: Snapshot Shows the Result of (000020-IM) After SBRG

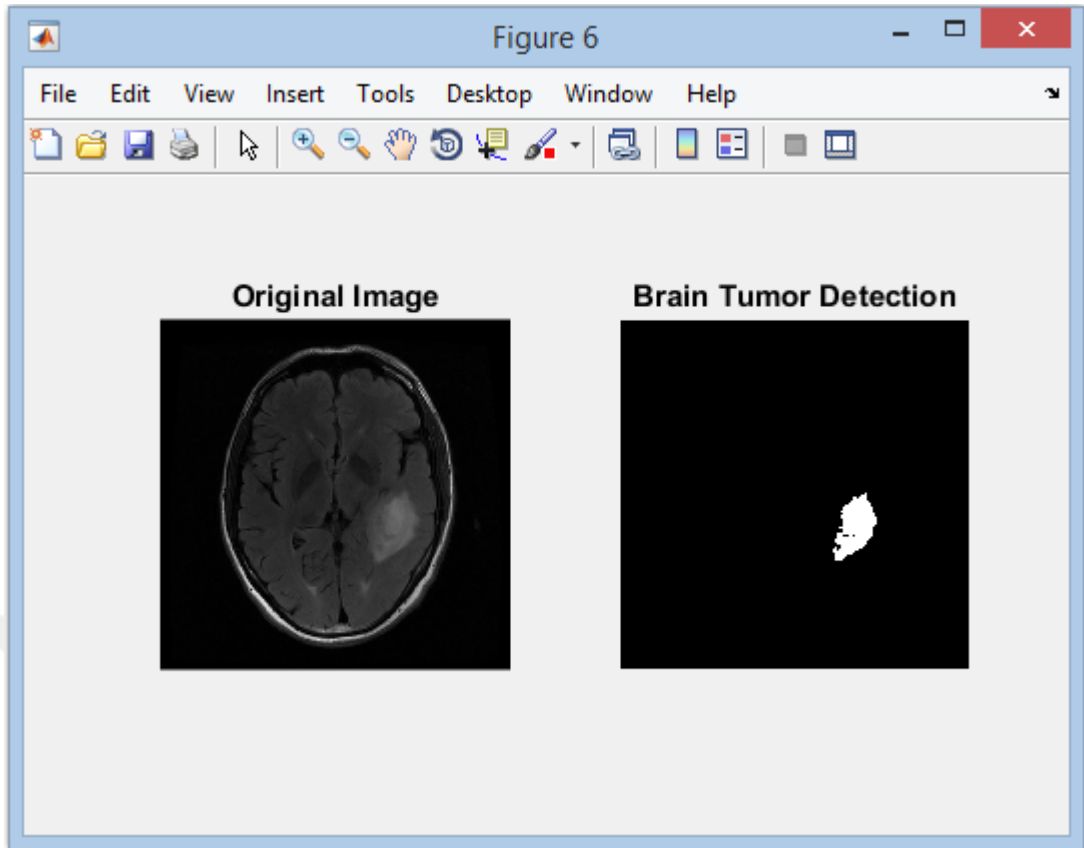


Figure 21: Snapshot Shows the Result of (000021-IM) After SBRG

A simple Graphical User Interface (GUI) was designed to display the result of our proposed system as follows:

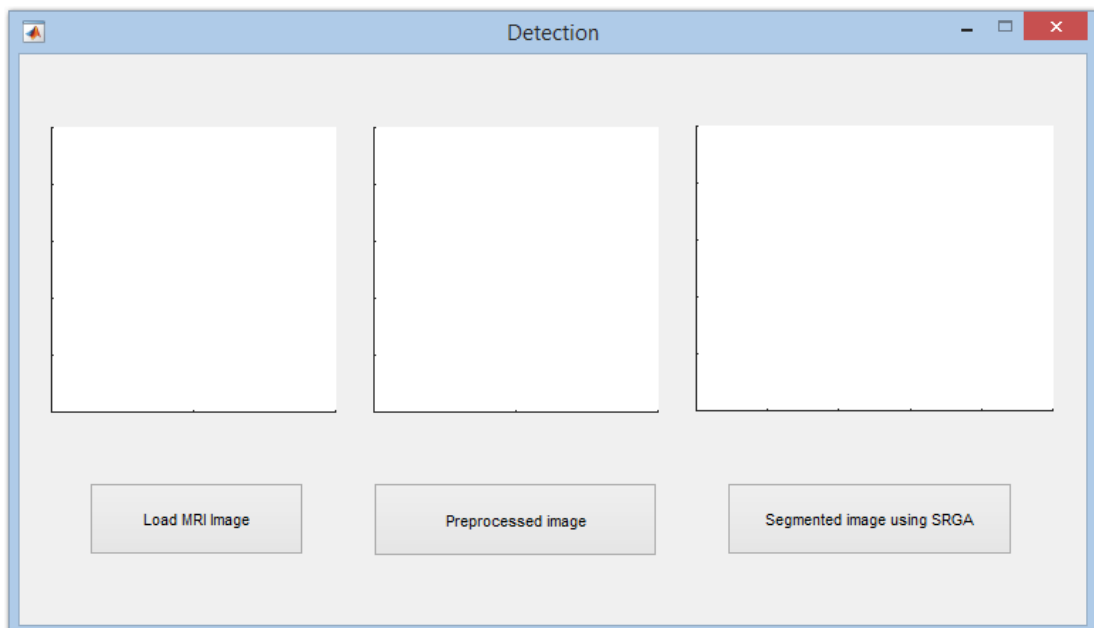


Figure 22: Design of Graphical User Interface 1

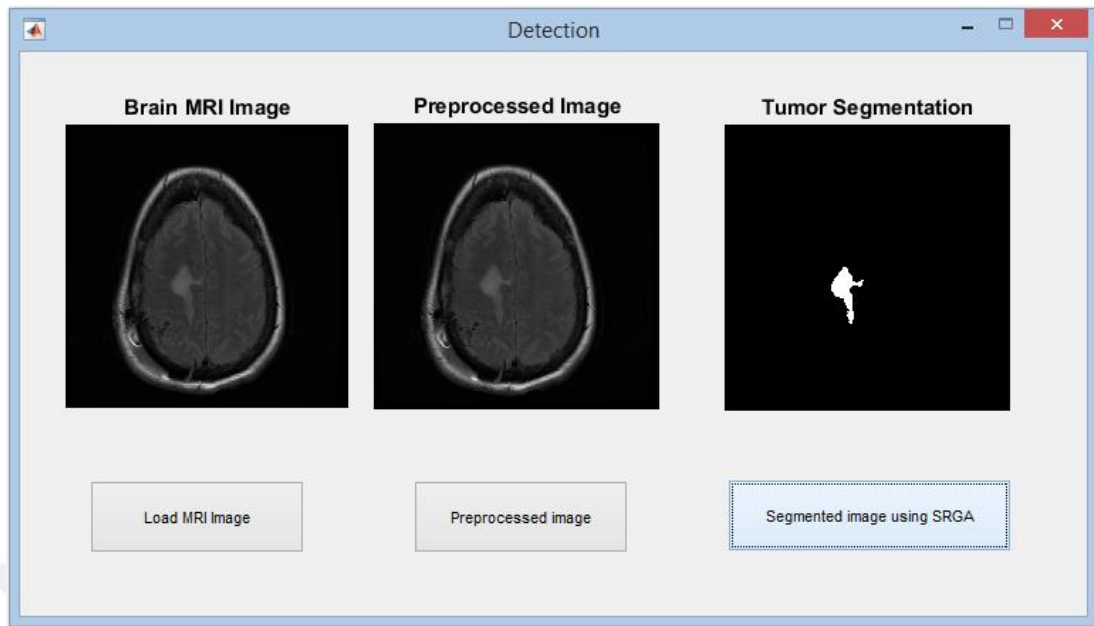


Figure 23: Design of Graphical User Interface 2

The Graphical User Interface works by first loading the MRI image, then preprocessing is performed and finally the region growing method is applied using the seed point obtained by the neural network classification stage.

4.3. Evaluation:

The system performance is evaluated in this step where the final segmentation result obtained based on both classification and region-growing implementation is compared with the ground truth of MRI image. Experimental performance evaluation is done by using Confusion Matrix, which calculates the different similarity metrics between the obtained result and its ground truth (binary image). The confusion matrix is shown in Figure (20) display the confusion matrix where in this section the evaluation will include all the pixels in the (512×512) binary image to make sure the tumor is determined accurately.

		Actual Value	
		positives	negatives
Predicted Value	positives	TP True Positive	FP False Positive
	negatives	FN False Negative	TN True Negative

Figure (24): Confusion Matrix

Confusion matrix elements definition:

TP: indicates the number of predicted pixels located as a tumor and they do have tumor.

TN: indicates the number of predicted pixels located as non-tumor and they don't have tumor.

FP: indicates the number of predicted pixels located as a tumor but they don't have a tumor.

FN: indicates the number of predicted pixels located as non-tumor but they actually do have tumor.

Evaluation Metrics:

$$\text{Accuracy} = \frac{TP+TN}{TP+FP+FN+TN}$$

$$\text{Precision} = \frac{TP}{TP+FP}$$

$$\text{Recall (Sensitivity)} = \frac{TP}{TP+FN}$$

$$\text{Specificity} = 1 - \frac{FP}{FP+TN}$$

The following Table (3) includes confusion matrix statistical values of comparing our segmentation result with the ground truth.

Table 3: Proposed System Statistical Values

IMAGE NO.	TP	FP	FN	TN	Total positive	Total negative
000001-IM	3972	5	546	257621	4518	257626
000005-IM	3175	0	402	258567	3577	258567
000014-IM	2449	135	60	259500	2509	259635
000018-IM	3015	68	122	258939	3137	259007
000025-IM	2145	15	174	259810	2319	259825

Next Table (4) includes calculation of the evaluation metrics obtained by the previous table.

Table 4: Calculation of Evaluation Metrics

IMAGE NO.	Accuracy	Precision	Recall (Sensitivity)	Specificity
000001-IM	0.9979	0.9987	0.8792	0.9999
000005-IM	0.9984	1	0.8876	1
000014-IM	0.9993	0.9478	0.9761	0.9994
000018-IM	0.9993	0.9779	0.9611	0.9997
000025-IM	0.9993	0.9931	0.925	0.9999

Finally the performance evaluation of our proposed system is gained by calculating the average for each of the Accuracy, Precision, Sensitivity, and Specificity in the previous Table:

Table 5: Evaluation of Proposed System

Evaluation Performance
Total Accuracy: 99.88%
Total Precision: 98.35%
Total Sensitivity: 92.58%
Total Specificity: 99.97%

A comparison of the performance evaluation of different segmentation and classification techniques showing the Accuracy, Sensitivity and Specificity for each method are given in the Table below.

Table 6: Comparison of Various Segmentation Methods

Authors	Segmentation Method	Accuracy	Sensitivity	Specificity
Proposed Method	Region Growing	99.88%	92.58%	99.97%
Maitra and Chatterjee(2006) [22]	ANN & SVM	100%	-	-
Synthuja et al. (2016) [23]	Region Growing	93.50%	91.06%	85.12%
Irshad and Jaffery (2015) [24]	Otsu	94.20%	1%	94%
	FCM	96.70%	1%	96%
	Region Growing	97.80%	57.60%	98.90%
Maitra and Chatterjee (2008) [25]	FCM	100%	-	-
El-Dahshan et al. (2010) [26]	ANN	97%	98.30%	90%
	K-NN	98.65%	100%	90%
Zacharaki et al. (2009) [27]	SVM	85%	87%	79%
Chaplot et al. (2006) [28]	DWT & SVM	98%	-	-

CHAPTER 5

CONCLUSION AND FUTURE WORK

5.1. Conclusion:

The brain tumor is a serious disease that has become widespread in recent years. The diagnosis of this disease and finding its exact location in the brain is considered as one of the difficult tasks in the medical field. In order to help doctors and physicians to facilitate their work many brain tumor detection systems have been designed using different image processing techniques to detect those tumors.

In this thesis a brain tumor detection system was designed and presented. The proposed system was able to determine the boundaries of the suspicious regions in MRI images with high precision achieving promising results.

At first the MRI image was preprocessed by normalizing the gray level input image in order to get accurate results. Then in the second stage the image was divided into blocks in order to calculate the 13 Haralick features and choose the most effective ones to be used in the next section. The following section was building a neural network based on the extracted features to classify the suspicious regions in the MRI image in order to make sure that seed point of the segmentation method is selected from the tumor area. After selecting the seed points the region growing algorithm was performed to detect the tumor.

In the performance evaluation the results of the segmentation method (extracted tumor) was compared with ground truth using the confusion matrix and therefore very accurate and precise results were gained.

The ratio of evaluation metrics achieved in our system was 99.88% of accuracy, 92.58% of Sensitivity, and 99.97% of Specificity.

5.2. Future Work:

As dealing with a system that detects a serious disease the accuracy and reliability are needed where the future plans should be focused on developing the system to make it able to work on different MRI images and also try to use different segmentation techniques to segment the tumor. Accordingly, we suggested the following recommendations:

- Developing the system to be able to distinguish the tumor after extraction if it is benign or malignant.
- Using different features that could be added to the Haralick feature to increase the performance of the classification stage.
- Try other segmentation technique for better performance and decreasing the number of FP errors.
- Improving the system so that it can distinguish between brain skull and the tumor which have same properties instead of selecting it manually.

REFERENCES

1. **American Cancer Society**, "Global Cancer Facts & Figures", from <http://www.cancer.org>. [Accessed: October. 29, 2017].
2. **Brain Tumour Research**. "Stark Facts", from <http://www.braintumourresearch.org>. [Accessed: October. 30, 2017].
3. **World Health Organization**, "Cancer Fact Sheet", February 2017, from <http://www.who.int>. [Accessed: October. 29, 2017].
4. **Diaz I, Boulanger P, Greiner R, Hoehn B, Rowe L and Murtha A (2013)**, "An Automatic Brain Tumor Segmentation Tool, " 35th Annual Intl. Conf. IEEE Eng. In Med. And Bio. Soc. (EMBC), pp. 3339-3342.
5. **D. Paternain, M. Pagola, J. Fernandez, R. Mesiar, G. Beliakov, and H. Bustince (2011)**, "Brain MRI thresholding using incomparability and overlap functions", in Intelligent Systems Design and Applications (ISDA), 11th International Conference, pp. 808-812.
6. **J. Kong, J. Wang, Y. Lu, J. Zhang, Y. Li, and B. Zhang (2006)**, "A novel approach for segmentation of MRI brain images" , in Electrotechnical Conference, IEEE Mediterranean, pp. 525-528.
7. **J. Wu, et al. (2008)**, "Texture Feature based Automated Seeded Region Growing in Abdominal MRI Segmentation," Proceedings of International Conference on Biomedical Engineering and Informatics, IEEE, pp. 263-267.
8. **R.M. Haralick, K. Shanmugam, and I. Dinstein (1973)**, "Texture Features for Image Classification", IEEE Trans. On Systems, Man, and Cybernetics, vol. Smc-3, no.6, pp. 610-621.

9. **W. Yang, M. Siliang (2011)**, “Automatic detection and segmentation of brain tumor using fuzzy classification and deformable models”, 4th International Conference on Biomedical Engineering and Informatics, IEEE, pp. 1680-1683.
10. **Nelly Gordillo, Eduard Montseny and Pilar Sobrevilla (2013)**, “State of the art survey on MRI brain tumor segmentation”, Elsevier, pp. 1-13.
11. **Ho S, Bullitt E, Gerig G (2002)**, “Level-set evolution with region competition: automatic 3-D segmentation of brain tumors”. In: Proceedings of the international conference pattern recognition, vol 1, pp. 532–535.
12. **Asra Aslam, Ekram Khan, and MM Sufyan Beg (2015)**, “Improved Edge Detection Algorithm for Brain Tumor Segmentation”, ELSEVIER, Procedia Computer Science, vol. 58, pp. 430-437.
13. **A. Kouhi, H. Seyedarabi, A. Aghazolzadeh (2011)**, "A Modified FCM Algorithm for MRI Brain Image Segmentation", 2011 7th Iranian Conference on Machine Vision and Image Processing, IEEE, pp. 1-5.
14. **Li-Hong Juang, Ming-Ni Wu (2010)**, “MRI brain lesion image detection based on color-converted K-means clustering segmentation”, ELSEVIER, Computer Science Section, vol.43, pp. 941-949.
15. **R.O. Duda, P.E. Hart (1973)**, Pattern Classification and Scene Analysis, Wiley, New York.
16. **S. Ruan et al (2007)**, “Tumor segmentation from a multispectral MRI images by using support vector machine classification“, In International Symposium on Biomedical Imaging, Washington, USA, pp. 1236–1239.
17. **Kishore K. Reddy, et al (2012)**, “Confidence Guided Enhancing Brain Tumor Segmentation in Multi-Parametric MRI”, 9th IEEE International Symposium on Biomedical Imaging, pp. 366-369.
18. **El-Sayed A. El-Dahshan, Heba M. Mohsen, Kenneth Revett, Abdel-Badeeh M. Salem (2014)**, “Computer-aided diagnosis of human brain tumor through

MRI: A survey and a new algorithm”, ELSEVIER, Expert Systems with Applications, pp. 5526–5545.

19. **Dipali M. Joshi, N. K. Rana, V. M. Misra (2010)**, “Classification of Brain Cancer Using Artificial Neural Network”, International Conference on Electronic Computer Technology, IEEE, pp. 112 -116.
20. **S.N. Deepa, and B.A. Devi (2012)**, “Artificial Neural Networks Design for Classification of Brain Tumour”, IEEE International Conference on Computer Communication and Informatics, pp. 1-6.
21. **The Cancer Imaging Archive (TCIA)**, from <http://www.cancerimagingarchive.net>. [Accessed: December. 19, 2017].
22. **Maitra, M., Chatterjee, A. (2006)**, A Slantlet transform based intelligent system for magnetic resonance brain image classification. Biomedical Signal Processing and Control, Elsevier, pp. 299-306.
23. **M.Mary Synthuja, Jain Preetha, Dr. L.Padma Suresh, M.John Bosco (2016)**, “FIREFLY BASED REGION GROWING AND REGION MERGING FOR IMAGE SEGMENTATION”, International Conference on Emerging Technological Trends (ICETT), IEEE, pp.1-9.
24. **Irshad, Zainul Abdin Jaffery (2015)**,"Performance comparison of image segmentation techniques for infrared images", IEEE, pp.1-5.
25. **Maitra, M., Chatterjee, A. (2008)**, “Hybrid multi resolution Slantlet transform and fuzzy c-means clustering approach for normal–pathological brain MR image segregation”, Medical Engineering and Physics, Elsevier, pp. 615–623.
26. **El-Sayed Ahmed El-Dahshana, Tamer Hosny and Abdel-Badeeh M.Salem (2010)**, "Hybrid intelligent techniques for MRI brain images classification", Elsevier, pp. 433-441.
27. **Evangelia I. Zacharaki, Sumei Wang, Sanjeev Chawla, Dong Soo Yoo, Ronald Wolf, Elias R. Melhem, and Christos Davatzikos (2009)**, Magnetic Resonance Medicine, pp. 1609-1618.

- 28. Chaplot, S., Patnaik, L. M., & Jagannathan, N. R. (2006), "Classification of magnetic resonance brain images using wavelets as input to support vector machine and neural network", Biomedical Signal Processing and Control, Elsevier, PP. 86–92.**



CURRICULUM VITAE

PERSONAL INFORMATION

Surname, name: ABUFARES, Anwar.

Date and Place of Birth: 23 May 1986, Libya.

Marital Status: Married.

Phone: 541 933 3199.

Email: Bufares.email@yahoo.com.

EDUCATION

Degree	Institution	Year of Graduation
M.Sc.	Çankaya Univ., Computer Engineering	2018
B.Sc.	Omar Al-Mukhtar Univ., Computer Science	2009
High School	King Fahd Academy	2005

WORK EXPERIENCE

Year	Place	Enrollment
2011	Omar Al-Mukhtar Univ. Department of Computer Science	Teaching Assistant

FOREIN LANGUAGES

English.

HOBBIES

Reading, Drawing, Photography.